

# Factorization Theorem Relating Euclidean and Light-Cone Parton Distributions

Taku Izubuchi,<sup>1,2</sup> Xiangdong Ji,<sup>3,4</sup> Luchang Jin,<sup>5,6</sup> Iain W. Stewart,<sup>7</sup> and Yong Zhao<sup>7</sup>

<sup>1</sup>*High Energy Accelerator Research Organization (KEK), Tsukuba 305-0801, Japan*

<sup>2</sup>*RIKEN-BNL Research Center, Brookhaven National Laboratory, Upton, NY 11973, USA*

<sup>3</sup>*Tsung-Dao Lee Institute, and College of Physics and Astronomy, Shanghai Jiao Tong University, Shanghai, 200240, P. R. China*

<sup>4</sup>*Maryland Center for Fundamental Physics, Department of Physics, University of Maryland, College Park, Maryland 20742, USA*

<sup>5</sup>*Physics Department, University of Connecticut, Storrs, Connecticut 06269-3046, USA*

<sup>6</sup>*RIKEN BNL Research Center, Brookhaven National Laboratory, Upton, NY 11973, USA*

<sup>7</sup>*Center for Theoretical Physics, Massachusetts Institute of Technology, Cambridge, MA 02139, USA*

In a large momentum nucleon state, the matrix element of a gauge-invariant Euclidean Wilson line operator accessible from lattice QCD can be related to the standard light-cone parton distribution function through the large-momentum effective theory (LaMET) expansion. This relation is given by a factorization theorem with a non-trivial matching coefficient. Using the operator product expansion we prove the large-momentum factorization of the quasi-parton distribution function in LaMET, and show that the more recently discussed Ioffe-time distribution approach also obeys an equivalent factorization theorem. Explicit results for the coefficients are obtained and compared at one-loop. Our proof clearly demonstrates that the matching coefficients in the  $\overline{\text{MS}}$  scheme depend on the large partonic momentum rather than the nucleon momentum.

## I. INTRODUCTION

Parton distribution functions (PDFs) are key quantities for gaining an understanding of hadron structure and for making predictions for the cross sections in high-energy scattering experiments. In QCD factorization theorems for hard scattering processes [1], the relevant PDFs are defined in terms of the nucleon matrix elements of light-cone correlation operators. For example, in dimensional regularization with  $d = 4 - 2\epsilon$ , the bare unpolarized quark PDF is

$$q(x, \epsilon) \equiv \int \frac{d\xi^-}{4\pi} e^{-ixP^+\xi^-} \langle P | \bar{\psi}(\xi^-) \gamma^+ U(\xi^-, 0) \psi(0) | P \rangle, \quad (1)$$

where  $x$  is the momentum fraction, the nucleon momentum  $P^\mu = (P^0, 0, 0, P^z)$ ,  $\xi^\pm = (t \pm z)/\sqrt{2}$  are the light-cone coordinates, and the Wilson line is

$$U(\xi^-, 0) = P \exp \left( -ig \int_0^{\xi^-} d\eta^- A^+(\eta^-) \right). \quad (2)$$

Most often the bare PDF is renormalized in the  $\overline{\text{MS}}$  scheme to obtain  $q(x, \mu)$ , and this renormalized PDF is used to make predictions for experiment. The relation is

$$q(x, \epsilon) = \int_x^1 \frac{dy}{y} Z^{\overline{\text{MS}}} \left( \frac{x}{y}, \epsilon, \mu \right) q(y, \mu), \quad (3)$$

where  $\mu$  is the renormalization scale, and we have suppressed the flavor indices in the renormalization constant  $Z^{\overline{\text{MS}}}$  and PDFs. In light-cone quantization with  $A^+ = 0$ , the  $\overline{\text{MS}}$  definition has an interpretation as a parton number density.

So far our main knowledge of the PDF is obtained from global fits to deep inelastic scattering and jet data, see for example [2–6]. On the other hand, calculating the PDF from first principles with QCD has been an attractive subject, which can for example provide access to spin and momentum distributions that are hard to determine experimentally. Several different approaches to this have been considered using the lattice theory which is a non-perturbative method to solve QCD. Since the lattice theory is defined in a discretized Euclidean space with imaginary time, it is very difficult to calculate Minkowskian quantities with real-time dependence such as the PDF. The first and most well explored option is calculating the moments of the PDF [7–11] that are matrix elements of local gauge-invariant operators. However, since the lattice regularization breaks  $O(4)$  rotational symmetry, the consequent mixing between operators of different dimensions makes it difficult to compute higher moments, which in practice has limited the amount of information that can be extracted from this approach. Method on improving this situation by restoring the rotational symmetry has been proposed in Ref. [12]. Other proposals include extracting the PDF from the hadronic tensor [13–16] and the forward Compton amplitude [17], possibly with flavor changing currents [18], and the more general “lattice cross sections” [19, 20]. Systematic lattice analyses of these approaches are under investigation.

In Ref [21] Ji proposed that the  $x$ -dependence of the PDF can be extracted from a Euclidean distribution on the lattice, which can be understood in the language of the large momentum effective theory (LaMET) [22]. This Euclidean distribution is referred to as the quasi-PDF, whose bare matrix element is defined using a spatial cor-

relation of quarks along the  $z$  direction,

$$\tilde{q}(x, P^z, \epsilon) \equiv \int_{-\infty}^{\infty} \frac{dz}{4\pi} e^{ixP^z z} \langle P | \bar{\psi}(z) \Gamma U(z, 0) \psi(0) | P \rangle, \quad (4)$$

where  $\Gamma = \gamma^z$ ,  $z^\mu = ze^\mu$ ,  $e^\mu = (0, 0, 0, 1)$ , and the Wilson line is

$$U(z, 0) = P \exp \left( -ig \int_0^z dz' A^z(z') \right). \quad (5)$$

For finite momentum  $P^z$ ,  $\tilde{q}(x, P^z, \epsilon)$  has support in  $-\infty < x < \infty$ . According to Ref. [23], for the quasi-PDF one could also replace  $\Gamma = \gamma^z$  by  $\Gamma = \gamma^0$  in Eq. (4) as both definitions reduce to the PDF under an infinite Lorentz boost along the  $z$  direction. Unlike the PDF in Eq. (1) that is invariant under the Lorentz boost, the quasi-PDF depends dynamically on it through the nucleon momentum  $P^z$ . When the nucleon momentum  $P^z$  is much larger than the nucleon mass  $M$  and  $\Lambda_{\text{QCD}}$ , which is an attainable window on the lattice, the quasi-PDF can be factorized into a matching coefficient and the PDF [21, 22]. The factorization theorem is

$$\tilde{q}(x, P^z, \mu_R) = \int_{-1}^1 \frac{dy}{|y|} C \left( \frac{x}{y}, \frac{\mu_R}{P^z}, \frac{\mu}{p^z} \right) q(y, \mu) + \mathcal{O} \left( \frac{M^2}{P_z^2}, \frac{\Lambda_{\text{QCD}}^2}{P_z^2} \right), \quad (6)$$

where the renormalized quasi-PDF  $\tilde{q}(x, P^z, \mu_R)$  is defined in a particular scheme at renormalization scale  $\mu_R$ , and  $\mathcal{O}(M^2/P_z^2, \Lambda_{\text{QCD}}^2/P_z^2)$  are higher-twist contributions suppressed by the nucleon momentum. In general the result for  $C$  will depend on the choice of  $\Gamma = \gamma^z$  or  $\gamma^0$ . For  $\Gamma = \gamma^z$  the matching coefficient  $C$  has been computed for the iso-vector quark quasi-PDF at one-loop level, first with a transverse momentum cutoff in [24], confirmed in [19, 25], and also recently determined in the  $\overline{\text{MS}}$  and RI/MOM schemes [26]. Matching for the gluon quasi-PDF is calculated in [27, 28]. The matching coefficient  $C$  is independent of the choice of states used for  $\tilde{q}$  and  $q$ .<sup>1</sup> Since matching calculations are carried out with quark states of momentum  $p^z$ , it can be tricky to know what the right choice to make is for  $C$ , and in some of the literature the choice of  $p^z = P^z$  has been adopted when utilizing  $C$  for the hadronic nucleon state. This is for example the case in the original quasi-PDF papers [21, 22, 24] and in the pioneering lattice calculations of the PDF from the quasi-PDF in [25, 29–36], which was summarized in Ref. [37]. In the quasi-generalized parton distribution analysis in [38] it was observed that

<sup>1</sup> The scheme definition itself may separately involve a choice of state, such as in the RI/MOM scheme, but the result is still an operator renormalization that can be used for different choices of hadronic states for  $\tilde{q}$  and  $q$ . The transverse cutoff and  $\overline{\text{MS}}$  schemes do not require even this choice.

Distribution	Fourier transform from Ioffe-time distribution	Arguments
Ioffe-time		$\zeta = zP^z, z^2$
Quasi-PDF	$z \rightarrow xP^z$	$x, P^z$
Pseudo-PDF	$\zeta \rightarrow x$	$x, z^2$

TABLE I. Summary of the relationship between different Euclidean distributions.

one should take  $p^z = |y|P^z$ . Through our rigorous derivation of Eq. (6) we prove that the correct choice for this equation is indeed  $p^z = |y|P^z$ .

Recently, a modified approach [39] to calculate PDFs from lattice QCD has been proposed based on using the Ioffe-time distribution (or pseudo-PDF), in place of the quasi-PDF. In this approach, one starts from the Ioffe-time distribution  $\tilde{Q}_{\gamma^\mu}$  defined for  $\mu = 0$  or  $\mu = z$  by

$$\frac{1}{2} \langle P | \tilde{O}_{\gamma^\mu}(z, \epsilon) | P \rangle = P^\mu \tilde{Q}_{\gamma^\mu}(\zeta = P^z z, z^2, \epsilon), \quad (7)$$

where  $\zeta = P^z z$  is the Ioffe time. For an arbitrary Dirac matrix  $\Gamma$  the operator  $\tilde{O}_\Gamma$  is defined as

$$\tilde{O}_\Gamma(z, \epsilon) = \bar{\psi}(z) \Gamma U(z, 0) \psi(0). \quad (8)$$

This is the same spatial correlation used to define the quasi-PDF in Eq. (4), where  $P^z$  is fixed and one Fourier transforms with respect to  $z$ . If instead  $z^2$  is fixed, and we Fourier transform from the Ioffe time  $\zeta$ —which is in principle integrating over  $P^z$ —to the momentum fraction  $x$ , then one obtains the pseudo-PDF [39],

$$\mathcal{P}(x, z^2, \epsilon) = \int_{-\infty}^{\infty} \frac{d\zeta}{2\pi} e^{ix\zeta} \tilde{Q}_{\gamma^0}(\zeta, z^2, \epsilon). \quad (9)$$

For arbitrary finite  $z$ , the pseudo-PDF only has support in  $-1 \leq x \leq 1$  [40, 41]. (Again the pseudo-PDF can equally well be considered for  $\Gamma = \gamma^z$ .) The Ioffe-time or pseudo-PDF approach has been explored on the lattice [42, 43], where the short distance factorization behavior was explored. The PDF is a special case of the pseudo-PDF when the correlation is light-like. Defining

$$Q(\zeta, \epsilon) = \tilde{Q}_{\gamma^+}(\zeta = -P^+ \xi^-, z^2 = 0, \epsilon) \quad (10)$$

as the Ioffe-time distribution that gives the PDF we have

$$q(y, \epsilon) = \int_{-\infty}^{\infty} \frac{d\zeta}{2\pi} e^{iy\zeta} Q(\zeta, \epsilon). \quad (11)$$

In short the quasi-PDF and pseudo-PDF are different representations of the Ioffe-time distribution, as summarized in Table. I.

It was pointed out in Ref. [44] that to obtain enough information to extract the PDF for the Ioffe-time distribution with small  $z^2$ , one has to do lattice calculations with large momenta  $P^z$ , which is the same requirement

as for the quasi-PDF. Ref. [44] also proposed that the renormalized pseudo-PDF satisfies the following small  $z^2$  factorization,

$$\mathcal{P}(x, z^2 \mu_R^2) = \int \frac{dy}{|y|} \mathcal{C}\left(\frac{x}{y}, \frac{\mu_R^2}{\mu^2}, z^2 \mu_R^2\right) q(y, \mu) + \mathcal{O}(z^2 \Lambda_{\text{QCD}}^2, z^2 M^2), \quad (12)$$

which they verified at order  $O(\alpha_s)$  for the unpolarized iso-vector case with  $\Gamma = \gamma^0$ . (Again the coefficient  $\mathcal{C}$  will depend on the choice of  $\Gamma = \gamma^0$  or  $\gamma^z$ .)

Here we prove factorization theorems for the quasi-PDF, Ioffe-time distribution and pseudo-PDF, and show that they are different representations of the same fundamental factorization theorem. Through our proof we derive the explicit form of the large  $P^z$  and small  $z^2$  factorization theorems in Eq.(6) and Eq. (12) respectively, as well as the relationship between the matching coefficients  $C$  and  $\mathcal{C}$ . Since the requirement for large  $P^z$  and small  $z^2$  is the same for both the quasi-PDF and pseudo-PDF approaches, there is in principle no fundamental difference in applying either one to lattice calculations of the proton matrix element of  $\tilde{O}_\Gamma(z)$ . Since there are practical implementation issues that differ, it is interesting to explore both approaches, which can be done utilizing the same lattice data.

The rest of this paper is organized as follows: In Sec. II, by using an operator product expansion (OPE) of  $\tilde{O}_\Gamma(z)$ , we derive the large  $P^z$  factorization of LaMET in Eq. (6) and small  $z^2$  factorization of the pseudo-PDF in Eq. (12). Our proof shows that one must take  $p^z = |y|P^z$  in Eq. (6), so the corresponding argument in  $C$  is  $\mu/(|y|P^z)$ . On the other hand, its dependence on  $\mu_R/P^z$  is related to the renormalization scheme, and one is free to pick this  $P^z$  to be the nucleon momentum, as was done for example in the RI/MOM scheme in [26]. (This OPE approach was used recently in Ref. [20] to prove the factorization theorem for the ‘‘lattice cross sections’’, and the OPE proof carried out here was done independently and first presented in Ref. [45].) In Sec. III, we calculate the Ioffe-time, pseudo-PDF, and quasi-PDF distributions and matching coefficients at one-loop in  $\overline{\text{MS}}$  and analyze the Fourier-transform relation between the quasi-PDF and pseudo-PDF. Unlike earlier results for the quasi-PDF in  $\overline{\text{MS}}$ , we also use dimensional regularization with minimal subtraction to renormalize divergences at  $x = \pm\infty$ . In Sec. IV, we discuss how renormalization schemes other than  $\overline{\text{MS}}$  are easily incorporated into the factorization formulas. In Sec. V we carry out a numerical analysis of the matching coefficients, by computing the convolution in Eq. (6) numerically using the PDF determined by global fits [4]. We show that the difference between using  $p^z = P^z$  and  $p^z = |y|P^z$  in Eq. (6) is an important effect, and that our  $\overline{\text{MS}}$  matching coefficients are insensitive to cutoffs in the convolution integral. In Sec. VI, we discuss the implications of our factorization proof for the lattice calculation of the PDF in both the quasi-PDF and pseudo-PDF approaches. Finally, we conclude in Sec. VII.

## II. FACTORIZATION FROM THE OPE

### A. OPE and Factorization for the Ioffe-time Distribution

The operator product expansion (OPE) is a technique to expand nonlocal operators with separation  $z^\mu$  in terms of local ones in the Euclidean limit of  $z^2 \rightarrow 0$ . The OPE can be applied to both bare regulated operators as well as renormalized operators, and our focus will be on the latter. For the gauge-invariant Wilson operator  $\tilde{O}_\Gamma(z)$ , it was proven that it can be multiplicatively renormalized in coordinate space as [46, 47]

$$\tilde{O}_\Gamma(z, \mu) = Z_{\psi, z} e^{\delta m |z|} \tilde{O}_\Gamma(z, \epsilon), \quad (13)$$

where  $\delta m$  captures the power divergence from the Wilson line self-energy,  $Z_{\psi, z}$  only depends on the end points  $z, 0$  and renormalizes the logarithmic divergences. For simplicity, in this section we take  $\Gamma = \gamma^z$  for Eq. (13).

In the  $\overline{\text{MS}}$  scheme, the power divergence vanishes, and the renormalized  $\tilde{O}_\Gamma(z, \mu)$  can be expanded in terms of local gauge-invariant operators as

$$\begin{aligned} \tilde{O}_{\gamma^z}(z, \mu) = & \sum_{n=0}^{\infty} \left[ C_n(\mu^2 z^2) \frac{(-iz)^n}{n!} e_{\mu_1} \cdots e_{\mu_n} O_1^{\mu_0 \mu_1 \cdots \mu_n}(\mu) \right. \\ & + C'_n(\mu^2 z^2) \frac{(-iz)^n}{n!} e_{\mu_1} \cdots e_{\mu_n} O_2^{\mu_0 \mu_1 \cdots \mu_n}(\mu) \\ & \left. + \text{higher-twist operators} \right], \quad (14) \end{aligned}$$

where  $\mu_0 = z$ ,  $C_n = 1 + O(\alpha_s)$  and  $C'_n = O(\alpha_s)$  are Wilson coefficients, and  $O_1^{\mu_0 \mu_1 \cdots \mu_n}(\mu)$  and  $O_2^{\mu_0 \mu_1 \cdots \mu_n}(\mu)$  are the only allowed traceless symmetric twist-2 quark and gluon operators at leading power in the OPE,

$$O_1^{\mu_0 \mu_1 \cdots \mu_n}(\mu) = Z_{n+1}^{qq} (\bar{\psi} \gamma^{(\mu_0} i D^{\mu_1} \cdots i D^{\mu_n)} \psi - \text{trace}), \quad (15)$$

$$O_2^{\mu_0 \mu_1 \cdots \mu_n}(\mu) = Z_{n+1}^{gg} (F^{(\mu_0 \rho} i D^{\mu_1} \cdots i D^{\mu_{n-1}} F_\rho^{\mu_n)} - \text{trace}).$$

Here  $Z_{n+1}^{ij} = Z_{n+1}^{ij}(\mu, \epsilon)$  are multiplicative  $\overline{\text{MS}}$  renormalization factors and  $(\mu_0 \cdots \mu_n)$  stands for the symmetrization of these Lorentz indices.

The above OPE is valid for the operator itself, where we implicitly constrain ourselves to the subspace of matrix elements for which the twist expansion is appropriate. In the iso-vector case, the mixing with the gluon operators is absent, which we will stick to for the rest of the paper. When  $O_1^{\mu_0 \mu_1 \cdots \mu_n}$  is evaluated in the nucleon state,

$$\langle P | O_1^{\mu_0 \mu_1 \cdots \mu_n} | P \rangle = 2a_{n+1}(\mu) (P^{\mu_0} P^{\mu_1} \cdots P^{\mu_n} - \text{trace}), \quad (16)$$

where  $a_{n+1}(\mu)$  is the  $(n+1)$ -th moment of the PDF,

$$a_{n+1}(\mu) = \int_{-1}^1 dx x^n q(x, \mu), \quad (17)$$

and the explicit expression of the trace term have been derived in Ref. [30, 48].

As pointed out in Ref. [44], to obtain enough information for the Ioffe distribution at  $|\zeta| = |P^z z| \sim 1$  at small  $z^2$ , we have to choose  $P^z$  large compared to the scale  $\Lambda_{\text{QCD}}$ . When  $P_z^2 \gg \{\Lambda_{\text{QCD}}^2, M^2\}$ , the trace terms in Eq.(16) are suppressed by powers of  $M^2/P_z^2$ , while the contributions from higher-twist operators in Eq. (14) are suppressed by powers of  $\Lambda_{\text{QCD}}^2/P_z^2$  or  $z^2\Lambda_{\text{QCD}}^2$ . Therefore, the twist-2 contribution is the leading approximation of the nucleon matrix element  $\langle P|\tilde{O}_{\gamma^z}(z)|P\rangle$  at large momentum. From now on we will drop all the higher-twist contributions from our discussion.

The Wilson coefficients  $C_n(\mu^2 z^2)$  in the OPE of  $\tilde{O}_{\gamma^z}(z)$  can be computed in perturbation theory for  $\mu \sim 1/z \gg \Lambda_{\text{QCD}}$ . In the  $\overline{\text{MS}}$  scheme, the  $C_n$  are log-singular near  $z^2 = 0$ , and so is  $\langle P|\tilde{O}_{\gamma^z}(z, \mu)|P\rangle$ . For this reason the  $x$ -moments of the quasi-PDF  $\tilde{q}(x, P^z, \mu)$  do not exist, and the quasi-PDF will not simply become the PDF in the infinite  $P^z$  limit. Instead, we need a factorization formula which matches the quasi-PDF to the PDF. In contrast, for the pseudo-PDF the moments do exist since we hold  $\mu^2 z^2$  fixed when taking the  $x$ -moment. However, we still need a factorization formula to match the pseudo-PDF to the PDF. We will comment further about this below.

Based on Eqs. (14-17), we can write down the leading-twist approximation to the Ioffe-time distribution as

$$\begin{aligned} \tilde{Q}_{\gamma^z}(\zeta, \mu^2 z^2) &= \sum_n C_n(\mu^2 z^2) \frac{(-i\zeta)^n}{n!} a_{n+1}(\mu) \\ &= \sum_n C_n(\mu^2 z^2) \frac{(-i\zeta)^n}{n!} \int_{-1}^1 dy y^n q(y, \mu). \end{aligned} \quad (18)$$

It should be noted that the only approximation we have made so far is ignoring the higher twist effects that are suppressed by small  $z^2$  and the large momentum  $P^z$  of the nucleon. In the limit of  $P_z^2 \gg M^2, \Lambda_{\text{QCD}}^2$ , we have  $P^0 \sim P^z$ , so even if  $\mu_0 = 0$  in Eq. (14), the leading approximation of  $\tilde{O}_{\gamma^0}(z)$  is still given by the twist-2 contributions in Eq. (18), just with modified coefficients  $C_n$ .

Based on the OPE results in Eq. (18), we can derive a factorization formula in coordinate space for the Ioffe-time distribution. First of all, let us define a function  $\mathcal{C}(\alpha, \mu^2 z^2)$ :

$$\mathcal{C}(\alpha, \mu^2 z^2) \equiv \int \frac{d\zeta}{2\pi} e^{i\alpha\zeta} \sum_n C_n(\mu^2 z^2) \frac{(-i\zeta)^n}{n!}. \quad (19)$$

From Eq. (18) and the renormalized analog of the Fourier transform relation in Eq. (9)  $\mathcal{C}(\alpha, \mu^2 z^2)$  corresponds to a pseudo-PDF in the special case where  $a_{n+1}(\mu) = 1$ . The analysis of Ref. [40, 41] implies that the support of  $\mathcal{C}(\alpha, \mu^2 z^2)$  is  $-1 \leq \alpha \leq 1$ . Noting that

$$\int d\alpha e^{-i\alpha(y\zeta)} \mathcal{C}(\alpha, \mu^2 z^2) = \sum_n C_n(\mu^2 z^2) \frac{(-i\zeta y)^n}{n!}, \quad (20)$$

we find from Eq. (18) that

$$\tilde{Q}(\zeta, \mu^2 z^2) = \int_{-1}^1 dy \int_{-1}^1 d\alpha e^{-i\alpha(y\zeta)} \mathcal{C}(\alpha, \mu^2 z^2) q(y, \mu). \quad (21)$$

Finally, using the inverse transform of the renormalized analog of Eq. (11),

$$Q(\zeta, \mu) = \int_{-1}^1 dy e^{-iy\zeta} q(y, \mu). \quad (22)$$

we obtain

$$\tilde{Q}(\zeta, \mu^2 z^2) = \int_{-1}^1 d\alpha \mathcal{C}(\alpha, \mu^2 z^2) Q(\alpha\zeta, \mu). \quad (23)$$

The result in Eq. (23) is the factorization formula for the spatial Ioffe-time distribution  $\tilde{Q}(\zeta, \mu^2 z^2)$  which expresses it in terms of the light-cone correlation  $Q(\zeta, \mu)$  that defines the PDF. It has the same structure as the factorization theorem for the Euclidean correlation used for the calculation of the pion distribution amplitude in Ref. [49, 50].

## B. Factorization for the quasi-PDF

The renormalized quasi-PDF is defined as a Fourier transform of the renormalized Ioffe-time distribution,

$$\tilde{q}\left(x, \frac{\mu}{P^z}\right) \equiv \int \frac{d\zeta}{2\pi} e^{ix\zeta} \tilde{Q}\left(\zeta, \frac{\mu^2 \zeta^2}{P_z^2}\right). \quad (24)$$

Note that we could use either  $\tilde{Q}_{\gamma^z}$  or  $\tilde{Q}_{\gamma^0}$  here. Using the result for the Ioffe-time distribution in Eq. (18) this gives

$$\begin{aligned} \tilde{q}\left(x, \frac{\mu}{P^z}\right) &= \int_{-1}^1 dy \left[ \int \frac{d\zeta}{2\pi} e^{ix\zeta} \sum_{n=0} C_n\left(\frac{\mu^2 \zeta^2}{P_z^2}\right) \frac{(-i\zeta)^n}{n!} y^n \right] q(y, \mu) \\ &= \int_{-1}^1 \frac{dy}{|y|} \left[ \int \frac{d\zeta}{2\pi} e^{i\frac{x}{y}\zeta} \sum_{n=0} C_n\left(\frac{\mu^2 \zeta^2}{(yP^z)^2}\right) \frac{(-i\zeta)^n}{n!} \right] q(y, \mu). \end{aligned} \quad (25)$$

Already, one can see that the matching kernel is a function of  $x/y$  and  $\mu^2/(|y|P^z)$ . We define the kernel as

$$C\left(\frac{x}{y}, \frac{\mu}{|y|P^z}\right) \equiv \int \frac{d\zeta}{2\pi} e^{i\frac{x}{y}\zeta} \sum_{n=0} C_n\left(\frac{\mu^2 \zeta^2}{(yP^z)^2}\right) \frac{(-i\zeta)^n}{n!}, \quad (26)$$

and then Eq. (25) can be rewritten as

$$\tilde{q}\left(x, \frac{\mu}{P^z}\right) = \int_{-1}^1 \frac{dy}{|y|} C\left(\frac{x}{y}, \frac{\mu}{|y|P^z}\right) q(y, \mu), \quad (27)$$

which is the  $\overline{\text{MS}}$  factorization formula for the quasi-PDF. This result implies that the factorization formula

in Eq. (6) must have  $p^z = |y|P^z$  for the quasi-PDF in the  $\overline{\text{MS}}$  scheme. We will show that this remains true for any quasi-PDF scheme in Sec. IV. This differs from the choice  $p^z = P^z$  which had been conjectured and used in the early papers on the quasi-PDF [21, 22, 24]. Physically the correct result in Eq. (27) can be understood as the fact that the matching coefficient is only sensitive to the perturbative partonic dynamics, and hence it is the magnitude of the partonic momentum  $|y|P^z$  which appears, rather than the hadronic momentum  $P^z$ .

### C. Factorization for the pseudo-PDF

The renormalized pseudo-PDF is the Fourier transform of the renormalized Ioffe-time distribution

$$\mathcal{P}(x, \mu^2 z^2) = \int_{-\infty}^{\infty} \frac{d\zeta}{2\pi} e^{ix\zeta} \tilde{Q}(\zeta, \mu^2 z^2). \quad (28)$$

Since both the pseudo-PDF and Ioffe-time distribution are multiplicatively renormalized, this follows immediately from Eq. (9). If we take Eq. (23) and Fourier transform the Ioffe-time distribution  $\tilde{Q}(\zeta, \mu^2 z^2)$  into the pseudo-PDF, and light-cone correlation  $Q(\alpha\zeta, \mu)$  into the PDF, then we immediately obtain the factorization theorem for the pseudo-PDF,

$$\begin{aligned} \mathcal{P}(x, z^2 \mu^2) &= \int_{|x|}^1 \frac{dy}{|y|} \mathcal{C}\left(\frac{x}{y}, \mu^2 z^2\right) q(y, \mu) \\ &+ \int_{-1}^{-|x|} \frac{dy}{|y|} \mathcal{C}\left(\frac{x}{y}, \mu^2 z^2\right) q(y, \mu), \end{aligned} \quad (29)$$

which is the small  $z^2$  factorization formula in Eq. (12). The upper and lower limits of the integrals in Eq. (29) follow immediately from the support  $-1 \leq \alpha \leq 1$  of the matching coefficient  $\mathcal{C}(\alpha, z^2 \mu^2)$ , and we recall that we also have  $-1 \leq x \leq 1$  for the pseudo-PDF on the LHS.

Since the range of  $x$  is bounded for the pseudo-PDF the terms in the series expansion of the exponential in Eq. (28) exist,

$$\tilde{Q}(\zeta, \mu^2 z^2) = \sum_{n=0}^{\infty} \int_{-1}^1 dx \frac{(-i\zeta)^n x^n}{n!} \mathcal{P}(x, \mu^2 z^2). \quad (30)$$

Comparing with Eq. (18) this implies that the moments of the pseudo-PDF are given by

$$\int_{-1}^1 dx x^n \mathcal{P}(x, \mu^2 z^2) = C_n(\mu^2 z^2) a_{n+1}(\mu). \quad (31)$$

So far we have proven the large  $P^z$  factorization of the quasi-PDF and small  $z^2$  factorization of the Ioffe-time and pseudo-PDFs. After deriving one factorization formula this immediately led to the others, since they are just different representations of the same spatial correlation function. Indeed, we see that the quasi-PDF and

pseudo-PDF are related at leading power by their definitions:

$$\tilde{q}\left(x, \frac{\mu}{P^z}\right) = \int \frac{d\zeta}{2\pi} e^{ix\zeta} \int_{-1}^1 dy e^{-iy\zeta} \mathcal{P}\left(y, \frac{\mu^2 \zeta^2}{P_z^2}\right), \quad (32)$$

where we have used  $z = \zeta/P^z$ . Based on Eq. (19) and Eq. (26), the Wilson coefficients in their factorization theorems also maintain the same relationship,

$$C\left(\xi, \frac{\mu}{|y|P^z}\right) = \int \frac{d\zeta}{2\pi} e^{i\xi\zeta} \int_{-1}^1 d\alpha e^{-i\alpha\zeta} \mathcal{C}\left(\alpha, \frac{\mu^2 \zeta^2}{(yP^z)^2}\right). \quad (33)$$

For the relations in Eqs. (32) and (33) the same choice of  $\Gamma = \gamma^0$  or  $\gamma^z$  should be used in the quasi- and pseudo-PDFs, or their corresponding coefficients.

In summary, there is a unique factorization formula that matches the quasi-PDF, Ioffe-time distribution and pseudo-PDF to the PDF. Since their factorizations into the PDF all require small distances and have nucleon large momentum, the setup for their lattice calculations must also be the same. Therefore, the LaMET and Ioffe-time (or pseudo) distribution approaches are in principle equivalent to each other, and they differ only by effects related to their implementation on the lattice.

In Ref. [39] it was speculated that one can study a ratio function

$$\tilde{Q}(\zeta, z^2, a^{-1})/\tilde{Q}(0, z^2, a^{-1}) \quad (34)$$

on a lattice with spacing  $a$ , and the  $O(z^2)$  corrections may cancel approximately. This idea was tested in Ref. [42] in lattice QCD, and the results show that the ratio is insensitive to  $z^2$  at small values. It is then interesting to consider what type of non-perturbative information can be extracted from this ratio.

This question can be answered using the small  $z^2$  factorization for the Ioffe-time distribution. According to Eq. (18),

$$\tilde{Q}(0, \mu^2 z^2) = C_0(\mu^2 z^2) + O(z^2 \Lambda_{\text{QCD}}^2), \quad (35)$$

where in the  $\overline{\text{MS}}$  scheme to one-loop [46, 51, 52]

$$C_0(\mu^2 z^2) = 1 + \frac{\alpha_s C_F}{2\pi} \left[ \frac{3}{2} \ln(\mu^2 z^2 e^{2\gamma_E}/4) + \frac{5}{2} \right]. \quad (36)$$

Then the ratio becomes

$$\begin{aligned} \frac{\tilde{Q}(\zeta, \mu^2 z^2)}{\tilde{Q}(0, \mu^2 z^2)} &= \sum_n \frac{C_n(\mu^2 z^2)}{C_0(\mu^2 z^2)} \frac{(-i\zeta)^n}{n!} a_{n+1}(\mu) \\ &+ O(z^2 \Lambda_{\text{QCD}}^2). \end{aligned} \quad (37)$$

Using Eq. (31) and our  $\overline{\text{MS}}$  one-loop perturbative pseudo-PDF result in Eq. (53) below we find for  $\Gamma = \gamma^0$  that

$$\begin{aligned} C_n(\mu^2 z^2) &= 1 + \frac{\alpha_s C_F}{2\pi} \left[ \left( \frac{3+2n}{2+3n+n^2} + 2H_n \right) \ln \frac{\mu^2 z^2 e^{2\gamma_E}}{4} \right. \\ &\left. + \frac{5+2n}{2+3n+n^2} + 2(1-H_n)H_n - 2H_n^{(2)} \right], \end{aligned} \quad (38)$$

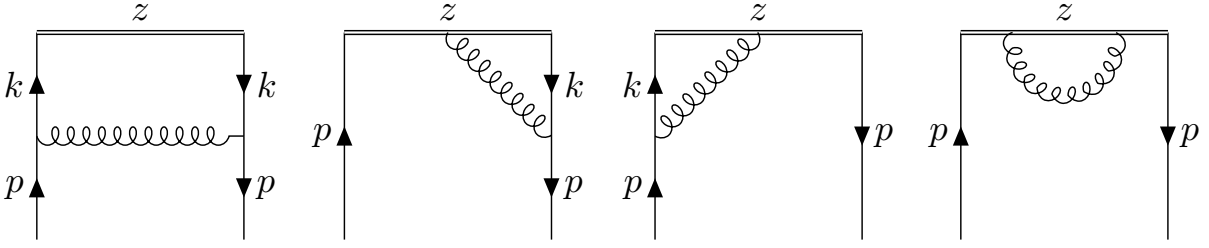


FIG. 1. One-loop Feynman diagrams for the quasi-PDF, Ioffe-time and pseudo-PDFs. The standard quark self energy wave-function is also included.

where the Harmonic numbers are  $H_n = \sum_{i=1}^n 1/i$  and  $H_n^{(2)} = \sum_{i=1}^n 1/i^2$ . For the case  $\Gamma = \gamma^z$  we have  $C_n^{\gamma^z}(\mu^2 z^2) = C_n(\mu^2 z^2) + \Delta C_n^{\gamma^z}(\mu^2 z^2)$  with

$$\Delta C_n^{\gamma^z}(\mu^2 z^2) = \frac{\alpha_s C_F}{2\pi} \frac{2}{2+3n+n^2}, \quad (39)$$

which also modifies Eq. (36) for  $n = 0$ . At small  $z^2$  where the perturbative expansion with  $\mu \simeq 1/z$  is valid, the ratio in Eq. (37) has a weak logarithmic dependence on  $|z|$ , which is consistent with the lattice findings in Refs. [42, 43]. The weak dependence on  $|z|$  can be quantitatively described by an evolution equation in  $\ln z^2$  [39, 53]. According to our OPE proof, here  $\tilde{Q}(0, \mu^2 z^2)$  only serves as an overall normalization factor which is contaminated by higher-twist corrections, and the  $\ln z^2$  evolution can be put in accurate terms with the factorization formula in Eq. (23) that enables us extract

the PDF from the ratio function.<sup>2</sup>

### III. EQUIVALENCE AT ONE-LOOP ORDER

As has been proven in Sec. II, the quasi-PDF and pseudo-PDF as well as their matching coefficients are related by a simple Fourier transform in Eq. (32) and Eq. (33). This relation is valid to all orders in perturbation theory. In this section we check the relations in Eq. (32) and Eq. (33) at one-loop order. We choose  $\Gamma = \gamma^0$  for our main presentation, but also quote final results for the case  $\Gamma = \gamma^z$ .

In the Feynman gauge, we calculate the quark matrix elements of the unpolarized iso-vector quasi-PDF, pseudo-PDF, and light-cone PDF at one-loop order in dimensional regularization with  $d = 4 - 2\epsilon$ . The external quark state is chosen to be on-shell and massless, and we regularize the UV and collinear divergences by  $1/\epsilon_{\text{UV}}$  ( $\epsilon_{\text{UV}} > 0$ ) and  $1/\epsilon_{\text{IR}}$  ( $\epsilon_{\text{IR}} < 0$ ) respectively. The one-loop order Feynman diagrams are shown in Fig. 1.

In an on-shell quark state with momentum  $p^\mu = (p^0 = p^z, 0, 0, p^z)$ , for  $\Gamma = \gamma^0$ , each diagram gives

$$\begin{aligned} \tilde{Q}_{\text{vertex}}^{(1)}(\zeta, z^2, \epsilon) &= \frac{\mu^{2\epsilon} \iota^\epsilon}{2p^0} \bar{u}(p) \int \frac{d^d k}{(2\pi)^d} (-igT^a \gamma^\mu) \frac{i}{\not{k}} \gamma^0 \frac{i}{\not{k}} (-igT^a \gamma^\nu) \frac{-ig_{\mu\nu}}{(p-k)^2} u(p) e^{-ik^z z}, \\ \tilde{Q}_{\text{sail}}^{(1)}(\zeta, z^2, \epsilon) &= \frac{\mu^{2\epsilon} \iota^\epsilon}{2p^0} \bar{u}(p) \int \frac{d^d k}{(2\pi)^d} (igT^a \gamma^0) \frac{1}{i(p^z - k^z)} \left( e^{-ip^z z} - e^{-ik^z z} \right) \delta^{\mu z} \frac{i}{\not{k}} (-igT^a \gamma^\nu) \frac{-ig_{\mu\nu}}{(p-k)^2} u(p) \\ &\quad + \frac{\mu^{2\epsilon} \iota^\epsilon}{2p^0} \bar{u}(p) \int \frac{d^d k}{(2\pi)^d} (-igT^a \gamma^\nu) \frac{i}{\not{k}} (igT^a \gamma^0) \frac{1}{i(p^z - k^z)} \left( e^{-ip^z z} - e^{-ik^z z} \right) \delta^{\mu z} \frac{-ig_{\mu\nu}}{(p-k)^2} u(p), \\ \tilde{Q}_{\text{tadpole}}^{(1)}(\zeta, z^2, \epsilon) &= \frac{\mu^{2\epsilon} \iota^\epsilon}{2p^0} \bar{u}(p) \int \frac{d^d k}{(2\pi)^d} (-g^2) C_F \gamma^0 \delta^{\mu z} \delta^{\nu z} \left( \frac{e^{-ip^z z} - e^{-ik^z z}}{(p^z - k^z)^2} - \frac{ze^{-ip^z z}}{i(p^z - k^z)} \right) \frac{-ig_{\mu\nu}}{(p-k)^2} u(p), \end{aligned} \quad (40)$$

where  $\iota = e^{\gamma_E}/(4\pi)$  is included to implement  $\mu$  in the  $\overline{\text{MS}}$  scheme,  $C_F = 4/3$ , and  $T^a$  is the SU(3) color matrix in the fundamental representation. The second term in the bracket in the last line, which is proportional  $z$ , does not contribute to the loop integral as it is odd under the exchange of  $p^z - k^z \rightarrow -(p^z - k^z)$ . The quark self-energy correction is  $\tilde{Q}_{\text{w.fn.}}^{(1)}(\zeta, z^2, \epsilon) = \delta Z_\psi \tilde{Q}^{(0)}(\zeta, z^2)$  with the tree level matrix element  $\tilde{Q}^{(0)}(\zeta, z^2) = e^{-i\zeta}$  and on-shell renormalization constant  $\delta Z_\psi$ ,

$$\delta Z_\psi = \frac{\alpha_s C_F}{2\pi} \left( -\frac{1}{2} \right) \left( \frac{1}{\epsilon_{\text{UV}}} - \frac{1}{\epsilon_{\text{IR}}} \right). \quad (41)$$

<sup>2</sup> The same point was demonstrated by work done very recently

in [52], which appeared simultaneously with our paper.

After carrying out the loop integrals in Eq. (40) according to the method in Ref. [44], we obtain

$$\begin{aligned}
\tilde{Q}_{\text{vertex}}^{(1)}(\zeta, z^2, \epsilon) &= \frac{\alpha_s C_F}{2\pi} e^{\epsilon\gamma_E} \int_0^1 du (1-\epsilon)(1-u) e^{-iu\zeta} \Gamma(-\epsilon) 4^{-\epsilon} (\mu|z|)^{2\epsilon} \\
&= \frac{\alpha_s C_F}{2\pi} e^{\epsilon\gamma_E} \left( \frac{\mu|z|}{2} \right)^{2\epsilon} \frac{(-1)\Gamma(2-\epsilon)}{\epsilon_{\text{IR}}} \frac{1-i\zeta - e^{-i\zeta}}{\zeta^2}, \\
\tilde{Q}_{\text{sail}}^{(1)}(\zeta, z^2, \epsilon) &= \frac{\alpha_s C_F}{2\pi} e^{\epsilon\gamma_E} \left[ (i\zeta) \int_0^1 du \int_0^1 dt (2-u) e^{-i(1-ut)\zeta} \Gamma(-\epsilon) 4^{-\epsilon} (t^2 z^2 \mu^2)^\epsilon \right. \\
&\quad \left. - \int_0^1 du e^{-iu\zeta} \Gamma(-\epsilon) 4^{-\epsilon} (z^2 \mu^2)^\epsilon + \left( \frac{1}{\epsilon_{\text{UV}}} - \frac{1}{\epsilon_{\text{IR}}} \right) e^{-i\zeta} \right] \\
&= \frac{\alpha_s C_F}{2\pi} e^{\epsilon\gamma_E} \left( \frac{\mu|z|}{2} \right)^{2\epsilon} \left\{ \frac{-\Gamma(1-\epsilon)}{\epsilon_{\text{IR}}} \frac{2(1-\epsilon)}{1-2\epsilon} \left[ \frac{1-e^{-i\zeta}}{-i\zeta} + e^{-i\zeta} (-i\zeta)^{-2\epsilon} (\Gamma(2\epsilon) - \Gamma(2\epsilon, -i\zeta)) \right] \right. \\
&\quad \left. + \frac{\Gamma(1-\epsilon)}{\epsilon_{\text{IR}}} \frac{e^{-i\zeta}}{\epsilon} + \left( \frac{1}{\epsilon_{\text{UV}}} - \frac{1}{\epsilon_{\text{IR}}} \right) e^{-i\zeta} \right\}, \\
\tilde{Q}_{\text{tadpole}}^{(1)}(\zeta, z^2, \epsilon) &= \frac{\alpha_s C_F}{2\pi} e^{\epsilon\gamma_E} \left( \frac{\mu|z|}{2} \right)^{2\epsilon} \frac{\Gamma(1-\epsilon)}{\epsilon_{\text{UV}}(1-2\epsilon)} e^{-i\zeta}.
\end{aligned} \tag{42}$$

For simplicity we have left out the tree level multiplicative spinor factor  $\bar{u}\gamma^0 u$  when quoting one-loop results in Eq. (42), and will continue to do so for the Ioffe-time, quasi-PDF, and pseudo-PDF results quoted below. Since  $\alpha_s^{\text{bare}} = \alpha_s(\mu)\mu^{2\epsilon} Z_g^2 = \alpha_s(\mu)\mu^{2\epsilon} + \mathcal{O}(\alpha_s^2)$  is  $\mu$ -independent we do not include  $\mu$  as an argument in the bare functions. In the final result for each term we have also specified whether  $1/\epsilon$  factors (that remain after expanding about  $\epsilon \rightarrow 0$ ) are IR or UV divergences. Combined with the wavefunction corection, the bare Ioffe-time distribution  $\tilde{Q}^{(1)}(\zeta, z^2, \epsilon)$  is

$$\begin{aligned}
\tilde{Q}^{(1)}(\zeta, z^2, \epsilon) &= \frac{\alpha_s C_F}{2\pi} e^{\epsilon\gamma_E} \left( \frac{\mu|z|}{2} \right)^{2\epsilon} \left\{ \frac{3}{2} \left( \frac{1}{\epsilon_{\text{UV}}} - \frac{1}{\epsilon_{\text{IR}}} \right) e^{-i\zeta} + \frac{(-1)\Gamma(2-\epsilon)}{\epsilon_{\text{IR}}} \left[ \frac{(1-i\zeta - e^{-i\zeta})}{\zeta^2} \right. \right. \\
&\quad \left. \left. + \frac{2}{1-2\epsilon} \left\{ \frac{1-e^{-i\zeta}}{-i\zeta} + e^{-i\zeta} (-i\zeta)^{-2\epsilon} (\Gamma(2\epsilon) - \Gamma(2\epsilon, -i\zeta)) - \frac{e^{-i\zeta}}{2\epsilon} \right\} \right] \right\}.
\end{aligned} \tag{43}$$

Note that as  $\epsilon \rightarrow 0$  the terms in the inner most curly brackets have no  $1/\epsilon$  term. Also we can verify that in the local limit of the operator that the bare one-loop correction vanishes as expected by conservation of the vector current:

$$\lim_{z \rightarrow 0} \tilde{Q}^{(1)}(zP^z, z^2, \epsilon) = \lim_{z \rightarrow 0} \frac{\alpha_s C_F}{2\pi} e^{\epsilon\gamma_E} \left( \frac{\mu|z|}{2} \right)^{2\epsilon} \left\{ \frac{3}{2} \left( \frac{1}{\epsilon_{\text{UV}}} - \frac{1}{\epsilon_{\text{IR}}} \right) + \frac{3}{2\epsilon_{\text{IR}}} \right\} = 0, \tag{44}$$

where we note that it is important that the  $1/\epsilon_{\text{IR}}$  terms cancel since the assumption  $\epsilon > 0$  is only valid for the  $1/\epsilon_{\text{UV}}$  term. The corresponding bare pseudo-PDF is

$$\begin{aligned}
\mathcal{P}^{(1)}(x, z^2, \epsilon) &= \frac{\alpha_s C_F}{2\pi} \left[ -1 + x + \frac{2}{(1-2\epsilon)} - \left( \frac{2}{(1-2\epsilon)} \frac{1}{(1-x)^{1-2\epsilon}} \right)_{+(1)}^{[0,1]} \right] e^{\epsilon\gamma_E} \left( \frac{\mu|z|}{2} \right)^{2\epsilon} \frac{\Gamma(2-\epsilon)}{\epsilon_{\text{IR}}} \theta(x)\theta(1-x) \\
&\quad + \frac{\alpha_s C_F}{2\pi} e^{\epsilon\gamma_E} \left( \frac{\mu|z|}{2} \right)^{2\epsilon} \frac{3}{2} \left( \frac{1}{\epsilon_{\text{UV}}} - \frac{1}{\epsilon_{\text{IR}}} \right) \delta(1-x).
\end{aligned} \tag{45}$$

Since we will encounter plus functions over different domains below, we define a plus function at  $x = x_0$  within a given domain  $D$  so that

$$\int_D dx [g(x)]_{+(x_0)}^D h(x) = \int_D dx g(x) [h(x) - h(x_0)]. \tag{46}$$

(See App. C for more details.) It is straightforward to confirm that the bare pseudo-PDF satisfies the local vector current conservation,  $\lim_{z \rightarrow 0} \int dx \mathcal{P}^{(1)}(x, z^2 \mu^2, \epsilon) = 0$ , with the same cancellation as in Eq. (44).

Now, according to the relations between the quasi-PDF and the Ioffe-time or pseudo-PDFs in Eqs. (24,32), we can do a Fourier or double Fourier transform of the results in Eqs. (43,45) to get the quasi-PDF. Despite its straightforwardness, the Fourier transform is subtle and the details are provided in App. A. Here we simply quote the result for

the bare quasi-PDF,

$$\begin{aligned} \tilde{q}^{(1)}(x, p^z, \epsilon) = & \frac{\alpha_s C_F}{2\pi} \left\{ \frac{3}{2} \left( \frac{1}{\epsilon_{UV}} - \frac{1}{\epsilon_{IR}} \right) \delta(1-x) + \frac{\Gamma(\epsilon + \frac{1}{2}) e^{\epsilon\gamma_E} \mu^{2\epsilon}}{\sqrt{\pi}} \frac{1-\epsilon}{p_z^{2\epsilon} \epsilon_{IR} (1-2\epsilon)} \right. \\ & \left. \times \left[ |x|^{-1-2\epsilon} \left( 1+x + \frac{x}{2}(x-1+2\epsilon) \right) - |1-x|^{-1-2\epsilon} \left( x + \frac{1}{2}(1-x)^2 \right) + I_3(x) \right] \right\}, \end{aligned} \quad (47)$$

where

$$I_3(x) = \theta(x-1) \left( \frac{x^{-1-2\epsilon}}{x-1} \right)_{+(1)}^{[1,\infty]} - \theta(x)\theta(1-x) \left( \frac{x^{-1-2\epsilon}}{1-x} \right)_{+(1)}^{[0,1]} - \delta(1-x) \pi \csc(2\pi\epsilon) + \theta(-x) \frac{|x|^{-1-2\epsilon}}{x-1}. \quad (48)$$

After some algebra one can confirm that the bare quasi-PDF satisfies local vector current conservation, with  $\int dx \tilde{q}^{(1)}(x, p^z, \epsilon) = 0$ . To verify this result one must carefully separate out  $1/\epsilon_{UV}$  factors arising from requiring  $\epsilon > 0$  to obtain convergence at  $x = \pm\infty$ , and  $1/\epsilon_{IR}$  factors that arise from requiring  $\epsilon < 0$  to obtain convergence at  $x = 1$ .

An alternate method of obtaining the quasi-PDF is to directly calculate it from the Feynman diagrams by first Fourier transforming  $z$  into  $xp^z$ . As a result, the factors  $(e^{-ip^z z} - e^{-ik^z z})$  are transformed into  $[\delta(p^z - xp^z) - \delta(k^z - xp^z)]$ , and all the loop integrals reduce to  $(d-1)$ -dimensional ones. This is the procedure for the matching calculations of the quasi-PDF used in Refs. [24, 26], and is distinct from doing the Fourier transformation after fully carrying out the integrals as in Eqs. (42–47). As a cross-check we have confirmed in App. B that we obtain the exactly same bare quasi-PDF in Eq. (47) from both procedures.

Now we consider the  $\epsilon$  expansion to obtain  $\overline{\text{MS}}$  renormalized results for the Ioffe-time, pseudo-PDF, and quasi-PDF. Expanding the Ioffe-time distribution in  $\epsilon$  we obtain

$$\tilde{Q}^{(1)}(\zeta, z^2, \epsilon) = \delta\tilde{Q}^{(1)}(\zeta, z^2, \mu, \epsilon_{UV}) + \tilde{Q}^{(1)}(\zeta, z^2, \mu, \epsilon_{IR}) + \mathcal{O}(\epsilon) \quad (49)$$

with the  $\overline{\text{MS}}$  counterterm and renormalized Ioffe-time distribution given by

$$\begin{aligned} \delta\tilde{Q}^{(1)}(\zeta, z^2, \mu, \epsilon_{UV}) &= \frac{\alpha_s C_F}{2\pi} e^{-i\zeta} \frac{3}{2} \frac{1}{\epsilon_{UV}}, \\ \tilde{Q}^{(1)}(\zeta, z^2, \mu, \epsilon_{IR}) &= \frac{\alpha_s C_F}{2\pi} \left\{ \frac{3}{2} \left( \ln \frac{\mu^2 z^2 e^{2\gamma_E}}{4} + 1 \right) e^{-i\zeta} + \left( -\frac{1}{\epsilon_{IR}} - \ln \frac{z^2 \mu^2 e^{2\gamma_E}}{4} - 1 \right) h(\zeta) + \frac{2(1-i\zeta - e^{-i\zeta})}{\zeta^2} \right. \\ &\quad \left. + 4i\zeta e^{-i\zeta} {}_3F_3(1, 1, 1, 2, 2, 2, i\zeta) \right\}. \end{aligned} \quad (50)$$

Here  ${}_3F_3$  is a hypergeometric function and the Fourier transform of  $[(1+x^2)/(1-x)]_{+(1)}^{[0,1]}$  gives the function

$$h(\zeta) = \frac{3}{2} e^{-i\zeta} + \frac{1+i\zeta - e^{-i\zeta} - 2i\zeta e^{-i\zeta}}{\zeta^2} - 2e^{-i\zeta} [\Gamma(0, -i\zeta) + \gamma_E + \ln(-i\zeta)]. \quad (51)$$

For the position space PDF we have

$$Q^{(1)}(\zeta, \mu, \epsilon_{IR}) = -\frac{\alpha_s C_F}{2\pi} \frac{1}{\epsilon_{IR}} h(\zeta). \quad (52)$$

Next we expand the bare pseudo-PDF from Eq. (45) in  $\epsilon$  to obtain the  $\overline{\text{MS}}$  counterterm and renormalized pseudo-PDF as  $\mathcal{P}^{(1)}(x, z^2, \epsilon) = \delta\mathcal{P}^{(1)}(x, z^2 \mu^2, \epsilon_{UV}) + \mathcal{P}^{(1)}(x, z^2 \mu^2, \epsilon_{IR}) + \mathcal{O}(\epsilon)$  with

$$\begin{aligned} \delta\mathcal{P}^{(1)}(x, z^2 \mu^2, \epsilon_{UV}) &= \frac{\alpha_s C_F}{2\pi} \frac{3}{2\epsilon_{UV}} \delta(1-x), \\ \mathcal{P}^{(1)}(x, z^2 \mu^2, \epsilon_{IR}) &= \frac{\alpha_s C_F}{2\pi} \left\{ \left( \frac{1+x^2}{1-x} \right)_{+(1)}^{[0,1]} \left[ -\left( \frac{1}{\epsilon_{IR}} + \ln \frac{e^{2\gamma_E}}{4} \right) - \ln(z^2 \mu^2) - 1 \right] - \left( \frac{4 \ln(1-x)}{1-x} \right)_{+(1)}^{[0,1]} + 2(1-x) \right\} \theta(x)\theta(1-x) \\ &\quad + \frac{\alpha_s C_F}{2\pi} \left[ \frac{3}{2} \ln(z^2 \mu^2) + \frac{3}{2} \ln \frac{e^{2\gamma_E}}{4} + \frac{3}{2} \right] \delta(1-x). \end{aligned} \quad (53)$$

Note that the renormalized  $\overline{\text{MS}}$  pseudo-PDF depends explicitly on  $\mu^2$ , and satisfies the relation to the renormalized  $\overline{\text{MS}}$  Ioffe-time distribution given in Eq. (28). It is also interesting to note that having expanded in  $\epsilon$ , local vector current conservation is no longer satisfied by the limit of the renormalized  $\overline{\text{MS}}$  pseudo-PDF, since

$$\lim_{z \rightarrow 0} \int dx \mathcal{P}^{(1)}(x, z^2 \mu^2, \epsilon_{\text{IR}}) \simeq (3\alpha_s C_F / 4\pi) \lim_{z \rightarrow 0} \ln(z^2 \mu^2) \quad (54)$$

gives a divergent result. The same divergence is present in the one-loop  $\overline{\text{MS}}$  renormalized Ioffe-time distribution in Eq. (50).

For the quasi-PDF there are two methods that we can consider for the renormalized calculation, either expanding the bare result in Eq. (47) and renormalizing in  $(x, p^z)$  space, or following our preferred definition in Eq. (24) and Fourier transforming the renormalized Ioffe-time distribution in Eq. (50). Although these two approaches will lead to the same final result for  $C$  for practical applications, there is a subtle difference that we will explain.

First consider the renormalization of the quasi-PDF done in  $(x, p^z)$  space. Expanding Eq. (47) in  $\epsilon$ , and writing  $\tilde{q}^{(1)}(x, p^z, \epsilon) = \delta\tilde{q}^{(1)}(x, \mu/|p^z|, \epsilon_{\text{UV}}) + \tilde{q}^{(1)}(x, \mu/|p^z|, \epsilon_{\text{IR}}) + \mathcal{O}(\epsilon)$  allows us to identify the  $\overline{\text{MS}}$  counterterm and renormalized quasi-PDF as

$$\begin{aligned} \delta\tilde{q}^{(1)}(x, \mu/|p^z|, \epsilon_{\text{UV}}) &= \frac{\alpha_s C_F}{2\pi} \frac{3}{2\epsilon_{\text{UV}}} \left[ \delta(1-x) - \frac{1}{2} \frac{1}{x^2} \delta^+\left(\frac{1}{x}\right) - \frac{1}{2} \frac{1}{(1-x)^2} \delta^+\left(\frac{1}{1-x}\right) \right], \\ \tilde{q}^{(1)}(x, \mu/|p^z|, \epsilon_{\text{IR}}) &= \frac{\alpha_s C_F}{2\pi} \begin{cases} \left( \frac{1+x^2}{1-x} \ln \frac{x}{x-1} + 1 + \frac{3}{2x} \right)_{+(1)}^{[1,\infty]} - \left( \frac{3}{2x} \right)_{+(\infty)}^{[1,\infty]} & x > 1 \\ \left( \frac{1+x^2}{1-x} \left[ -\frac{1}{\epsilon_{\text{IR}}} - \ln \frac{\mu^2}{4p_z^2} + \ln(x(1-x)) \right] - \frac{x(1+x)}{1-x} \right)_{+(1)}^{[0,1]} & 0 < x < 1 \\ \left( -\frac{1+x^2}{1-x} \ln \frac{-x}{1-x} - 1 + \frac{3}{2(1-x)} \right)_{+(1)}^{[-\infty,0]} - \left( \frac{3}{2(1-x)} \right)_{+(-\infty)}^{[-\infty,0]} & x < 0 \end{cases} \\ &+ \frac{\alpha_s C_F}{2\pi} \left[ \delta(1-x) - \frac{1}{2} \frac{1}{x^2} \delta^+\left(\frac{1}{x}\right) - \frac{1}{2} \frac{1}{(1-x)^2} \delta^+\left(\frac{1}{1-x}\right) \right] \left( \frac{3}{2} \ln \frac{\mu^2}{4p_z^2} + \frac{5}{2} \right). \end{aligned} \quad (55)$$

The details of working out the  $\epsilon$  expansion of Eq. (47) are provided in App. C, including definitions of the plus functions and  $\delta$ -functions at  $x_0 = \pm\infty$  that appear in the result quoted here. The  $\overline{\text{MS}}$  quasi-PDF obtained in Eq. (55) still satisfies vector current conservation

$$\int dx \tilde{q}^{(1)}(x, \mu/|p^z|, \epsilon_{\text{IR}}) = 0. \quad (56)$$

This is obviously the case for the plus function terms which individually integrate to zero, and is also true for the combination of  $\delta$ -functions which appears in Eq. (55).

The renormalized  $\overline{\text{MS}}$  quasi-PDF in Eq. (55) differs slightly from that obtained using our definition in Eq. (24). Using Eq. (24) and the renormalized Ioffe-time distribution in Eq. (50) we instead obtain

$$\begin{aligned} \delta\tilde{q}'^{(1)}(x, \mu/|p^z|, \epsilon_{\text{UV}}) &= \frac{\alpha_s C_F}{2\pi} \frac{3}{2\epsilon_{\text{UV}}} \delta(1-x), \\ \tilde{q}'^{(1)}(x, \mu/|p^z|, \epsilon_{\text{IR}}) &= \frac{\alpha_s C_F}{2\pi} \begin{cases} \left( \frac{1+x^2}{1-x} \ln \frac{x}{x-1} + 1 + \frac{3}{2x} \right)_{+(1)}^{[1,\infty]} - \left( \frac{3}{2x} \right)_{+(\infty)}^{[1,\infty]} & x > 1 \\ \left( \frac{1+x^2}{1-x} \left[ -\frac{1}{\epsilon_{\text{IR}}} - \ln \frac{\mu^2}{4p_z^2} + \ln(x(1-x)) \right] - \frac{x(1+x)}{1-x} \right)_{+(1)}^{[0,1]} & 0 < x < 1 \\ \left( -\frac{1+x^2}{1-x} \ln \frac{-x}{1-x} - 1 + \frac{3}{2(1-x)} \right)_{+(1)}^{[-\infty,0]} - \left( \frac{3}{2(1-x)} \right)_{+(-\infty)}^{[-\infty,0]} & x < 0 \end{cases} \\ &+ \frac{\alpha_s C_F}{2\pi} \left[ \delta(1-x) \left( \frac{3}{2} \ln \frac{\mu^2}{4p_z^2} + \frac{5}{2} \right) + \frac{3}{2} \gamma_E \left( \frac{1}{(x-1)^2} \delta^+\left(\frac{1}{x-1}\right) + \frac{1}{(1-x)^2} \delta^+\left(\frac{1}{1-x}\right) \right) \right]. \end{aligned} \quad (57)$$

To carry out this calculation we defined the Fourier transformation of the singular function  $\ln(\zeta^2)$  as

$$\begin{aligned} \int \frac{d\zeta}{2\pi} e^{ix\zeta} \ln \zeta^2 &= \left[ \frac{d}{d\eta} \int \frac{d\zeta}{2\pi} e^{ix\zeta} (\zeta^2)^\eta \right] \Big|_{\eta=0} = \left[ \frac{d}{d\eta} \frac{4^\eta}{\Gamma(-\eta)} \frac{\Gamma(\eta+1/2)}{\sqrt{\pi}} \frac{[\theta(x) + \theta(-x)]}{|x|^{1+2\eta}} \right] \Big|_{\eta=0} \\ &= \gamma_E \left[ \left( -\delta(x) + \frac{1}{x^2} \delta^+ \left( \frac{1}{x} \right) \right) + \left( -\delta(x) + \frac{1}{x^2} \delta^+ \left( \frac{1}{-x} \right) \right) \right] \\ &\quad - \left[ \left( \frac{1}{x} \right)_{+(0)}^{[0,1]} + \left( \frac{1}{x} \right)_{+(\infty)}^{[1,\infty]} \right] \theta(x) - \left[ \left( \frac{1}{-x} \right)_{+(0)}^{[-1,0]} + \left( \frac{1}{-x} \right)_{+(\infty)}^{[-\infty,-1]} \right] \theta(-x), \end{aligned} \quad (58)$$

where we have used the results in Eqs. (A1,C7) to derive the second and last equalities, and took the limit  $\eta \rightarrow 0^+$  or  $\eta \rightarrow 0^-$  when needed. This  $\tilde{q}^{(1)}(x, \mu/|p^z|, \epsilon_{\text{IR}})$  does not satisfy vector-current conservation, and is different from  $\tilde{q}^{(1)}(x, \mu/|p^z|, \epsilon_{\text{IR}})$  in Eq. (55) only by the  $\delta$ -functions at  $x_0 = \pm\infty$ . Within the function domain  $-\infty < x < \infty$ , they are exactly the same.

The final ingredient we need for the matching calculations is the PDF, whose one-loop bare matrix element can be written as a sum of an  $\overline{\text{MS}}$  counterterm and renormalized matrix element,  $q^{(1)}(x, \epsilon) = \delta q^{(1)}(x, \epsilon_{\text{UV}}) + q^{(1)}(x, \epsilon_{\text{IR}})$ , where

$$\begin{aligned} \delta q^{(1)}(x, \epsilon_{\text{UV}}) &= \frac{\alpha_s C_F}{2\pi} \frac{1}{\epsilon_{\text{UV}}} \left( \frac{1+x^2}{1-x} \right)_{+(1)}^{[0,1]} \theta(x) \theta(1-x), \\ q^{(1)}(x, \epsilon_{\text{IR}}) &= \frac{\alpha_s C_F}{2\pi} \frac{(-1)}{\epsilon_{\text{IR}}} \left( \frac{1+x^2}{1-x} \right)_{+(1)}^{[0,1]} \theta(x) \theta(1-x). \end{aligned} \quad (59)$$

With the above results in hand we can now determine the matching coefficients up to one-loop order. Using Eq. (29) we find

$$\mathcal{C}^{(1)}(\alpha, z^2 \mu^2) = \mathcal{P}^{(1)}(\alpha, z^2 \mu^2, \epsilon_{\text{IR}}) - q^{(1)}(\alpha, \epsilon_{\text{IR}}). \quad (60)$$

Therefore the matching coefficient relating the pseudo-PDF and PDF in the  $\overline{\text{MS}}$  scheme with  $\Gamma = \gamma^0$  is<sup>3</sup>

$$\begin{aligned} \mathcal{C}(\alpha, z^2 \mu^2) &= \left[ 1 + \frac{\alpha_s C_F}{2\pi} \left( \frac{3}{2} \ln(z^2 \mu^2) + \frac{3}{2} \ln \frac{e^{2\gamma_E}}{4} + \frac{3}{2} \right) \right] \delta(1-\alpha) \\ &\quad + \frac{\alpha_s C_F}{2\pi} \left\{ \left( \frac{1+\alpha^2}{1-\alpha} \right)_{+(1)}^{[0,1]} \left[ -\ln(z^2 \mu^2) - \ln \frac{e^{2\gamma_E}}{4} - 1 \right] - \left( \frac{4 \ln(1-\alpha)}{1-\alpha} \right)_{+(1)}^{[0,1]} + 2(1-\alpha) \right\} \theta(\alpha) \theta(1-\alpha). \end{aligned} \quad (61)$$

This result is independent of the infrared regulator as it must be. We have also computed the matching coefficient for  $\Gamma = \gamma^z$  case, and it is  $\mathcal{C}_{\gamma^z}(\alpha, z^2 \mu^2) = \mathcal{C}(\alpha, z^2 \mu^2) + \Delta \mathcal{C}_{\gamma^z}(\alpha, z^2 \mu^2)$  with

$$\Delta \mathcal{C}_{\gamma^z}(\alpha, z^2 \mu^2) = \frac{\alpha_s C_F}{2\pi} 2(1-\alpha) \theta(\alpha) \theta(1-\alpha). \quad (62)$$

From Eq. (27) the corresponding relation for the matching coefficient for the quasi-PDF defined in Eq. (24) is

$$\mathcal{C}^{(1)}(\xi, \mu/(|y|P^z)) = \tilde{q}^{(1)}(\xi, \mu/|y|P^z, \epsilon_{\text{IR}}) - q^{(1)}(\xi, \epsilon_{\text{IR}}). \quad (63)$$

<sup>3</sup> While this work was being finalized, a one-loop analysis of the Ioffe-time distribution in the coordinate space appeared in Refs. [53, 54]. Our factorization result for the Ioffe-time distribution in Eq. (23) has a similar form to the hard part of the reduced Ioffe-time distribution found in Eq.(3.35) of Ref. [53] and Eq.(17) of Ref. [54]. While the precise definition of our  $\mathcal{C}(\alpha, z^2 \mu^2)$  and

this hard part may not be the same, it is interesting to note that our  $\overline{\text{MS}}$  result in Eq. (61) differs from Ref. [53, 54] due to the presence of our  $\delta(1-\alpha)$  terms, and a difference in the  $2(1-\alpha)$  term. Our result for  $\mathcal{C}(\alpha, z^2 \mu^2)$  should be used to extract an  $\overline{\text{MS}}$  PDF from an  $\overline{\text{MS}}$  result for the pseudo-PDF.

Therefore the matching coefficient relating the quasi-PDF and PDF is

$$C\left(\xi, \frac{\mu}{|y|P^z}\right) = \delta(1-\xi) + \frac{\alpha_s C_F}{2\pi} \begin{cases} \left(\frac{1+\xi^2}{1-\xi} \ln \frac{\xi}{\xi-1} + 1 + \frac{3}{2\xi}\right)_{+(1)}^{[1,\infty]} - \left(\frac{3}{2\xi}\right)_{+(\infty)} & \xi > 1 \\ \left(\frac{1+\xi^2}{1-\xi} \left[-\ln \frac{\mu^2}{y^2 P_z^2} + \ln(4\xi(1-\xi))\right] - \frac{\xi(1+\xi)}{1-\xi}\right)_{+(1)}^{[0,1]} & 0 < \xi < 1 \\ \left(-\frac{1+\xi^2}{1-\xi} \ln \frac{-\xi}{1-\xi} - 1 + \frac{3}{2(1-\xi)}\right)_{+(1)}^{[-\infty,0]} - \left(\frac{3}{2(1-\xi)}\right)_{+(-\infty)}^{[-\infty,0]} & \xi < 0 \end{cases} \\ + \frac{\alpha_s C_F}{2\pi} \left[ \delta(1-\xi) \left(\frac{3}{2} \ln \frac{\mu^2}{4y^2 P_z^2} + \frac{5}{2}\right) + \frac{3}{2} \gamma_E \left(\frac{1}{(\xi-1)^2} \delta^+\left(\frac{1}{\xi-1}\right) + \frac{1}{(1-\xi)^2} \delta^+\left(\frac{1}{1-\xi}\right)\right) \right]. \quad (64)$$

Again this result is independent of the IR regulator as it must be. Here the plus function terms  $[g_1(\xi)]_{+(1)}^{[1,\infty]}$  and  $[g_2(\xi)]_{+(1)}^{[-\infty,0]}$  have integrands that converge for  $\xi \rightarrow \pm\infty$ , behaving as  $g_i(\xi) \sim 1/\xi^2$ . Note that if we had instead use the renormalized  $\overline{\text{MS}}$  quasi-PDF calculated in Eq. (55), we will obtain a different matching coefficient  $C$  with different  $\delta$ -functions at  $\xi = \pm\infty$ . However, the  $\delta$ -functions do not contribute to the convolution integral in Eq. (27) for any integrable PDFs. For example, to carry out the convolution with  $1/\xi^2 \delta^+(1/\xi)$  we can use  $\delta^+(\frac{1}{\xi}) = \lim_{\beta \rightarrow 0^+} \delta(\frac{1}{\xi} - \beta)$ , which when plugged into the factorization formula gives

$$\lim_{\beta \rightarrow 0^+} \int \frac{dy y^2}{|y| x^2} \delta\left(\frac{y}{x} - \beta\right) f_{u-d}(y) = \lim_{\beta \rightarrow 0^+} \beta f_{u-d}(\beta x). \quad (65)$$

For the plus-function at  $\infty$  using Eqs. (C9) and (C3) we have

$$\int_{-1}^{+1} \frac{dy}{|y|} \left[\frac{1}{(x/y)}\right]_{+(\infty)}^{[1,\infty]} f_{u-d}(y) = \lim_{\beta \rightarrow 0^+} \int_{-1}^{+1} \frac{dy}{|y|} \left[\frac{\theta(x/y - \beta)}{x/y} + \frac{y^2}{x^2} \delta\left(\frac{y}{x} - \beta\right) \ln \beta\right] f_{u-d}(y) \\ = \int_{-1}^{+1} \frac{dy}{|y|} \frac{y}{x} f_{u-d}(y) + \lim_{\beta \rightarrow 0^+} \beta f_{u-d}(\beta x) \ln \beta.$$

In the last line we dropped the  $\theta(x/y - \beta)$  since at small  $y$  our PDF behaves as  $f_{u-d}(y) \sim y^{-1+a}$  with  $0 < a < 1$ . This also implies

$$\lim_{\beta \rightarrow 0} \beta f_{u-d}(\beta x) \propto x^{-1+a} \lim_{\beta \rightarrow 0} \beta^a = 0, \\ \lim_{\beta \rightarrow 0} \beta f_{u-d}(\beta x) \ln \beta \propto x^{-1+a} \lim_{\beta \rightarrow 0} \beta^a \ln \beta = 0, \quad (66)$$

which means that the distribution contributions evaluated at  $\xi = \pm\infty$  in the matching coefficient  $C$  give zero contribution.

Therefore, the matching coefficients calculated from the quasi-PDFs in Eq. (55) and Eq. (57) are the same in effect, and we can simply drop all the  $\delta$ -functions at  $\xi = \pm\infty$  when plugging them into the factorization formula:

$$C^{\overline{\text{MS}}}\left(\xi, \frac{\mu}{|y|P^z}\right) = \delta(1-\xi) + \frac{\alpha_s C_F}{2\pi} \begin{cases} \left(\frac{1+\xi^2}{1-\xi} \ln \frac{\xi}{\xi-1} + 1 + \frac{3}{2\xi}\right)_{+(1)}^{[1,\infty]} - \frac{3}{2\xi} & \xi > 1 \\ \left(\frac{1+\xi^2}{1-\xi} \left[-\ln \frac{\mu^2}{y^2 P_z^2} + \ln(4\xi(1-\xi))\right] - \frac{\xi(1+\xi)}{1-\xi}\right)_{+(1)}^{[0,1]} & 0 < \xi < 1 \\ \left(-\frac{1+\xi^2}{1-\xi} \ln \frac{-\xi}{1-\xi} - 1 + \frac{3}{2(1-\xi)}\right)_{+(1)}^{[-\infty,0]} - \frac{3}{2(1-\xi)} & \xi < 0 \end{cases} \\ + \frac{\alpha_s C_F}{2\pi} \delta(1-\xi) \left(\frac{3}{2} \ln \frac{\mu^2}{4y^2 P_z^2} + \frac{5}{2}\right). \quad (67)$$

The use of Eq. (67) in the factorization theorem is valid for any PDF that behaves as  $\lim_{y \rightarrow 0} f(y, \mu) \sim y^{-1+a}$  with  $a > 0$ . We have also computed the matching coefficient for the  $\Gamma = \gamma^z$  case, and it is given by  $C_{\gamma^z}(\xi, \mu/(|y|P^z)) = C(\xi, \mu/(|y|P^z)) + \Delta C_{\gamma^z}(\xi, \mu/(|y|P^z))$  with

$$\Delta C_{\gamma^z}(\xi, \mu/(|y|P^z)) = \frac{\alpha_s C_F}{2\pi} 2(1-\xi). \quad (68)$$

Our result for  $C^{\overline{\text{MS}}}$  with  $\Gamma = \gamma^z$  agrees with Ref. [26], up to our different treatment of the UV divergences of the quasi-PDF at  $x = \pm\infty$  in  $\overline{\text{MS}}$  which leads to the presence of plus-functions and  $\delta$ -functions at  $\xi = \pm\infty$  in Eq. (64). In Ref. [26], the logarithmic UV divergent behavior  $\sim 1/x$  of the quasi-PDF at  $x = \pm\infty$  appeared in the  $x = 1$  plus-function (corresponding to canceling the two  $3/(2\xi)$  and  $3/(2(1-\xi))$  terms that appear in different plus functions in Eq. (64)). Here these divergences were subtracted in  $\overline{\text{MS}}$  yielding the plus functions and  $\delta$ -functions at  $\xi = \pm\infty$ . We will see in Sec. V that the correct result in Eq. (67) leads to convergent convolution integrals, in contrast with the  $\overline{\text{MS}}$  result of Ref. [26].

Since the renormalized pseudo-PDF and quasi-PDF satisfy the relation in Eq. (32) by definition,  $C(\xi, \mu/(|y|P^z))$  and  $\mathcal{C}(\alpha, z^2\mu^2)$  that are given by Eqs. (61, 64) automatically satisfy the relation in Eq. (33). This concludes our discussion of the equivalence between the quasi-PDF and pseudo-PDF at one-loop order.

#### IV. OTHER RENORMALIZATION SCHEMES

Although we derive the above matching formula assuming that the quasi-PDF is renormalized in the  $\overline{\text{MS}}$  scheme, this is not a limitation to our result. Since the gauge-invariant Wilson line operator  $\tilde{O}_\Gamma(z)$  has been proven to be multiplicatively renormalizable in the coordinate space [46, 47], one can convert  $\tilde{Q}_\Gamma(z)$  from any other scheme to the  $\overline{\text{MS}}$  scheme before using the above factorization formula. The renormalization of the quasi-PDF has been studied in many recent papers [26, 28, 33, 34, 51, 55–59]. We will discuss some of these results and show how they can be incorporated into the factorization formula in Eq. (27).

The  $\overline{\text{MS}}$  scheme is convenient for our discussion of the OPE as it guarantees Lorentz and gauge invariances, but it is not practical for lattice renormalization. Since the lattice theory has a natural UV cut-off  $1/a$  with  $a$  being the lattice spacing, the unrenormalized Ioffe-time distribution  $\tilde{Q}$  inherits the power divergence from the Wilson line self-energy according to Eq. (13). For an arbitrary scheme  $X$ , the renormalized Ioffe-time distribution

$$\tilde{Q}^X(\zeta, z^2\mu_R^2) = \lim_{a \rightarrow 0} Z_X^{-1}(z^2\mu_R^2, a^2\mu_R^2) \tilde{Q}(\zeta, z^2/a^2) \quad (69)$$

should be free of all the UV divergences and have a well-defined continuum limit as  $a \rightarrow 0$ . This continuum limit, in particular, is independent of the UV regulator, so

$$\begin{aligned} & \lim_{a \rightarrow 0} Z_X^{-1}(z^2\mu_R^2, a^2\mu_R^2) \tilde{Q}(\zeta, z^2/a^2) \\ &= Z_X^{-1}(z^2\mu_R^2, \epsilon) \tilde{Q}(\zeta, z^2, \epsilon). \end{aligned} \quad (70)$$

As a result, we can relate  $\tilde{Q}^X(\zeta, z^2\mu_R^2)$  to the  $\overline{\text{MS}}$  scheme by the conversion

$$\begin{aligned} \tilde{Q}^X(\zeta, z^2\mu_R^2) &= \frac{Z_{\overline{\text{MS}}}(\epsilon, \mu)}{Z_X(z^2\mu_R^2, \epsilon)} \tilde{Q}^{\overline{\text{MS}}}(\zeta, z^2\mu^2) \\ &= Z'_X(z^2\mu_R^2, \mu_R^2/\mu^2) \tilde{Q}^{\overline{\text{MS}}}(\zeta, z^2\mu^2), \end{aligned} \quad (71)$$

where the regulator  $\epsilon$  dependence is completely canceled out between  $Z_{\overline{\text{MS}}}$  and  $Z_X$ . The ratio  $Z'_X$  can be calculated perturbatively in QCD, which was done in [51] for several lattice schemes and the RI/MOM scheme. Thus the factorization theorem we have proven in Sec. II still applies to  $\tilde{Q}^X$  with a slight modification to the coefficient

function,

$$\tilde{Q}^X(\zeta, z^2\mu_R^2) = \int_{-1}^1 d\alpha \mathcal{C}^X(\alpha, \mu_R^2/\mu^2, \mu^2 z^2) Q(\alpha\zeta, \mu), \quad (72)$$

where the matching coefficient for the scheme  $X$  is related to that of  $\overline{\text{MS}}$  by

$$\mathcal{C}^X(\alpha, \mu_R^2/\mu^2, \mu^2 z^2) = Z'_X(z^2\mu_R^2, \mu_R^2/\mu^2) \mathcal{C}(\alpha, \mu^2 z^2). \quad (73)$$

For the pseudo-PDF the modified result also involves this same coefficient

$$\begin{aligned} \mathcal{P}^X(x, z^2\mu_R^2) &= \int_{|x|}^1 \frac{dy}{|y|} \mathcal{C}^X\left(\frac{x}{y}, \frac{\mu_R^2}{\mu^2}, \mu^2 z^2\right) q(y, \mu) \\ &+ \int_{-1}^{-|x|} \frac{dy}{|y|} \mathcal{C}^X\left(\frac{x}{y}, \frac{\mu_R^2}{\mu^2}, \mu^2 z^2\right) q(y, \mu). \end{aligned} \quad (74)$$

Meanwhile, for the quasi-PDF we have,

$$\begin{aligned} \tilde{q}_X\left(x, \frac{\mu_R^2}{P_z^2}\right) &\equiv \int \frac{d\zeta}{2\pi} e^{ix\zeta} \tilde{Q}^X\left(\zeta, \frac{\mu^2 \zeta^2}{P_z^2}\right) \\ &= \int_{-1}^1 \frac{dy}{|y|} \mathcal{C}^X\left(\frac{x}{y}, \frac{\mu_R}{\mu}, \frac{\mu}{|y|P_z}\right) q(y, \mu). \end{aligned} \quad (75)$$

Here the modified coefficient for the  $X$  scheme is related to coefficient in the  $\overline{\text{MS}}$  scheme by

$$\begin{aligned} \mathcal{C}^X\left(\frac{x}{y}, \frac{\mu_R}{\mu}, \frac{\mu}{|y|P_z}\right) \\ = \int d\eta \bar{Z}'_X\left(\eta^2, \frac{\mu_R^2}{\mu^2}\right) \mathcal{C}\left(\frac{x}{y} - \frac{\eta}{|y|} \frac{\mu_R}{P_z}, \frac{\mu}{|y|P_z}\right), \end{aligned} \quad (76)$$

where here  $\bar{Z}'_X$  is defined by the Fourier transform

$$\bar{Z}'_X\left(\eta^2, \frac{\mu_R^2}{\mu^2}\right) \equiv \int \frac{d\tau}{2\pi} e^{i\eta\tau} Z'_X\left(\tau^2, \frac{\mu_R^2}{\mu^2}\right). \quad (77)$$

Depending on the scheme  $X$  we note that slightly modified definitions of  $\bar{Z}'_X$  may be more appropriate.

Besides the  $\overline{\text{MS}}$  scheme, the quasi-PDF has also been renormalized in the transverse momentum cut-off [19, 24, 25, 29] and regularization-invariant momentum subtraction (RI/MOM) [26, 33, 34, 51, 59] schemes. The

RI/MOM scheme has attracted strong interest recently as it can be implemented nonperturbatively on the lattice, so we consider it as an explicit example of the above relations. In this scheme, the renormalization constant  $Z_{\text{OM}}$  is determined by imposing a condition on the Ioffe-time distribution in an off-shell quark state,

$$\begin{aligned} Z_{\text{OM}}^{-1} \tilde{Q}(\zeta = zp^z, z^2/a^2, -p^2 a^2) \Big|_{p^2 = -\mu_R^2, p^z = p_R^z} \\ = \tilde{Q}_q^{(0)}(zp_R^z, z^2/a^2, z^2 \mu_R^2) = e^{-izp_R^z}, \end{aligned} \quad (78)$$

where  $q$  denotes the quark state,  $p^\mu$  is the external momentum, and “(0)” in the superscript stands for the tree-level matrix element. As a result,

$$\begin{aligned} Z_{\text{OM}} &= Z_{\text{OM}}(zp_R^z, z^2/a^2, a^2 \mu_R^2), \\ Z'_{\text{OM}} &= Z'_{\text{OM}}(zp_R^z, z^2 \mu_R^2, \mu_R^2/\mu^2), \end{aligned} \quad (79)$$

and here we define

$$\begin{aligned} \bar{Z}'_{\text{OM}} \left( \eta, \frac{\mu_R^2}{(p_R^z)^2}, \frac{\mu_R^2}{\mu^2} \right) \\ \equiv p_R^z \int \frac{dz}{2\pi} e^{i\eta p_R^z} Z'_{\text{OM}}(zp_R^z, z^2 \mu_R^2, \mu_R^2/\mu^2). \end{aligned} \quad (80)$$

Then the matching coefficient in Eq. (75) becomes

$$\begin{aligned} C^{\text{OM}} \left( \frac{x}{y}, \frac{\mu_R}{p_R^z}, \frac{\mu_R}{\mu}, \frac{\mu}{yP^z} \right) \\ = \int d\eta \bar{Z}'_{\text{OM}} \left( \eta, \frac{\mu_R^2}{(p_R^z)^2}, \frac{\mu_R^2}{\mu^2} \right) C \left( \frac{x}{y} - \frac{\eta p_R^z}{y P^z}, \frac{\mu}{|y|P^z} \right). \end{aligned} \quad (81)$$

The choices of  $\mu_R$  and  $p_R^z$  are independent of  $\mu$  and  $P^z$ , and  $p_R^z = P^z$  was used in Refs. [26, 34].

It should be noted that on the lattice, due to the breaking of chiral symmetry, the vector-like quark Wilson line operator  $\tilde{O}_{\gamma\mu}(z)$  can mix with the scalar operator  $\tilde{O}_1(z)$ , as has been discussed in Refs. [33, 34, 51, 59, 60]. After considering the mixing effects, the same factorization formula can still be applied to the RI/MOM quasi-PDF from lattice QCD.

## V. NUMERICAL RESULTS

In this section we numerically analyze the quasi-PDF, Ioffe-time distribution and pseudo-PDF by studying how the matching coefficients in Eqs. (27,29) change the PDF. The quasi-PDF has already been studied in this manner for the  $\overline{\text{MS}}$ , transverse momentum cut-off, and RI/MOM schemes in Ref. [26]. Our  $\overline{\text{MS}}$  result in Eq. (67) corrects the result found earlier in Ref. [26], and leads to stable convolution integrals. We also compare the differences between using hadron momentum  $p^z = P^z$  and the parton momentum  $p^z = |y|P^z$  for the matching coefficient in the  $\overline{\text{MS}}$  scheme. We take  $\Gamma = \gamma^0$  for the results here.

As an example we use for our analysis the unpolarized iso-vector parton distribution,

$$f_{u-d}(x, \mu) = f_u(x, \mu) - f_d(x, \mu) - f_{\bar{u}}(-x, \mu) + f_{\bar{d}}(-x, \mu), \quad (82)$$

where we include  $f_{\bar{u}}(-x, \mu) = -f_{\bar{u}}(x, \mu)$  and  $f_{\bar{d}}(-x, \mu) = -f_{\bar{d}}(x, \mu)$ , the anti-parton distributions. For ease of comparison, we use the next-to-leading-order iso-vector PDF  $f_{u-d}$  from MSTW 2008 [4] with the corresponding running coupling  $\alpha_s(\mu)$ .

To implement the plus functions in the numerical calculation, we impose a soft cutoff  $|y-x| < 10^{-m}$  and test the sensitivity of results to  $m$ . Since the limit of  $y \rightarrow 0$  corresponds to the asymptotic region  $|x/y| \rightarrow \infty$ , we also impose a UV cutoff  $|y| > 10^{-n}$  to test the convergence of the convolution integral. We find that all the results presented below are insensitive to  $m$  and  $n$ . The fact that our result in Eq. (67) has terms outside the plus function at 1 in each of the  $\xi \in [1, \infty]$  and  $\xi \in [-\infty, 0]$  intervals is important for ensuring that our  $\overline{\text{MS}}$  result for  $C$  is insensitive to the  $|y| > 10^{-n}$  cutoff. This was not the case for the definition of the  $\overline{\text{MS}}$  quasi-PDF used in [26] and is also not the case for the quasi-PDF that was defined with a transverse momentum cutoff [24]. The RI/MOM scheme result [26] does not suffer from this issue.

In Fig. 2 we compare the PDF with the quasi-PDF in the  $\overline{\text{MS}}$  scheme obtained from the convolution in Eq. (27) using our one-loop result in Eq. (67). We observe that changing from  $p^z = P^z$  to the correct  $p^z = |y|P^z$  shifts the result in the physical region by a considerable amount.

The same type of comparison can be made for the pseudo-PDF in the  $\overline{\text{MS}}$  scheme by applying the factorization formula in Eq. (29) and matching coefficient in Eq. (61). In Fig. 3a we compare the PDF and pseudo-PDF and their dependence on the factorization scale  $\mu$ , while in Fig. 3b we include the dependence of the pseudo-PDF on the distance  $|z|$ . Since the matching coefficient in Eq.(61) is similar to the parton splitting function except for the nontrivial finite constants, matching the PDF to the pseudo-PDF is analogous to evolving the PDF from  $\mu$  to the scale of  $1/|z|$ . This evolution has been calculated in Refs. [39]. The variation of  $|z|$  has a similar effect to the PDF evolution, as is observed in the right panel of Fig. 3. When  $|z|\mu = 1$ , the logarithm is zero, and the matching effect from  $\mathcal{C}$  is determined by the nontrivial constants in Eq.(61), which shifts the PDF downward in the large  $x$  region and upward in the small  $x$  region.

Finally, we can make a similar comparison for the Ioffe-time distribution in the  $\overline{\text{MS}}$  scheme obtained with Eq. (23) and Eq. (61). Its real and imaginary parts are even and odd functions of  $\zeta$  respectively, and are shown in Fig. 4. Again we show the residual dependence on  $\mu$  and  $|z|$  which are similar to that for the pseudo-PDF. The matching broadens the curves in the Ioffe-time space. The Ioffe-time distribution renormalized in the  $\overline{\text{MS}}$  scheme does not exhibit vector current (or particle number) conservation, which can be clearly seen from the fact that the real part of the distribution is not equal to 1 at  $\zeta = 0$  (except for the special case where  $|z|\mu$  is tuned to cancel the constant terms in the one-loop  $\mathcal{C}$ ).

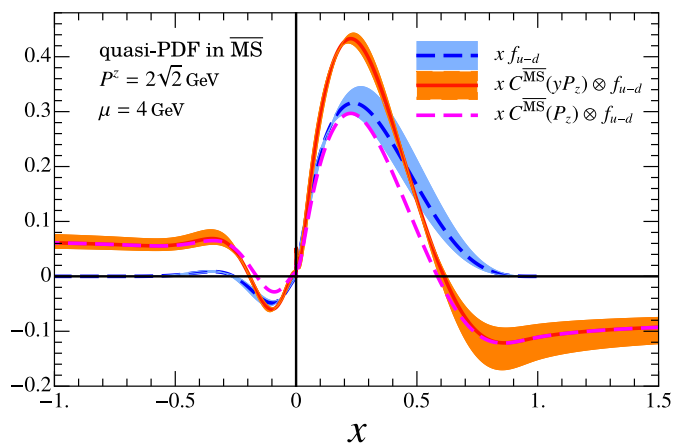


FIG. 2. The  $\overline{\text{MS}}$  scheme PDF  $x f_{u-d}$  and the  $\overline{\text{MS}}$  quasi-PDF obtained from  $x C^{\overline{\text{MS}}}(p^z) \otimes f_{u-d}$ , comparing results obtained with  $p^z = yP^z$  and  $p^z = P^z$ .

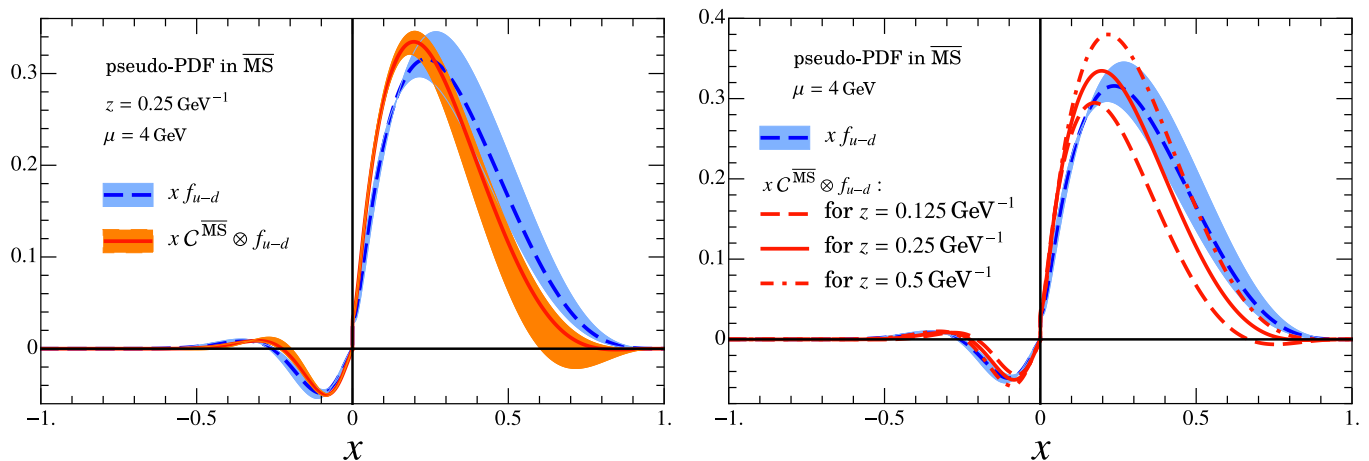


FIG. 3. (left) Comparison between the PDF  $x f_{u-d}$  and the pseudo-PDF  $x(C^{\overline{\text{MS}}} \otimes f_{u-d})$  in the  $\overline{\text{MS}}$  scheme. The orange and blue bands indicate the results from varying the factorization scale  $\mu = 4 \text{ GeV}$  by a factor of two. (right) Same but now showing only central pseudo-PDF curves for different values of  $z$ .

## VI. IMPLICATIONS FOR LATTICE CALCULATIONS

Our proof in Sec. II makes clear the relationship between the renormalized quasi-PDF, Ioffe-time, and pseudo-PDF distributions. As a practical matter there are a few different ways in which these equations can be used to convert a lattice calculation of the Ioffe-time distribution  $\tilde{Q}$  into a PDF. Three examples are 1) first Fourier transform to the quasi-PDF with Eq. (24), and then use the factorization theorem in Eq. (27), 2) first Fourier transform to the pseudo-PDF with Eq. (28), and then use the factorization theorem in Eq. (29), and 3) first match to the Fourier transform the position space PDF  $Q(\zeta, \mu)$  using the Ioffe-time factorization theorem in Eq. (23), and then transform it to the PDF with the inverse of Eq. (22). Since the numerical implementation of these steps may have slightly different systematics it

is interesting to compare them, or to use more than one approach in order to reduce uncertainties.

According to the analysis in Sec. II, for the factorization theorem of the Euclidean distributions to work, one must calculate the same correlation function, or Ioffe-time distribution, with small distance  $z^2$  and large momentum  $P^z$  so that the dynamical and kinematic higher-twist effects are suppressed. For practical lattice calculations, this means that there is only a finite number of useful data points in  $(z, P^z)$  that we can use to extract the PDF.

To illustrate this, consider a  $48^3 \times 64$  lattice with spacing  $a = 0.09 \text{ fm}$ . The distance of the spatial correlation  $z$  is in units of  $a \sim 1/2.2 \text{ GeV}^{-1}$ , and the nucleon momentum  $P^z$  is in units of  $2\pi/(48a) \sim 0.29 \text{ GeV}$ . Let us take  $\Lambda_{\text{QCD}} \sim 0.3 \text{ GeV}$ . In principle the target mass corrections can be subtracted. If we consider various values  $z = ma$  and  $P^z = n * 2\pi/(48a)$  for integer  $m$  and  $n$ , then

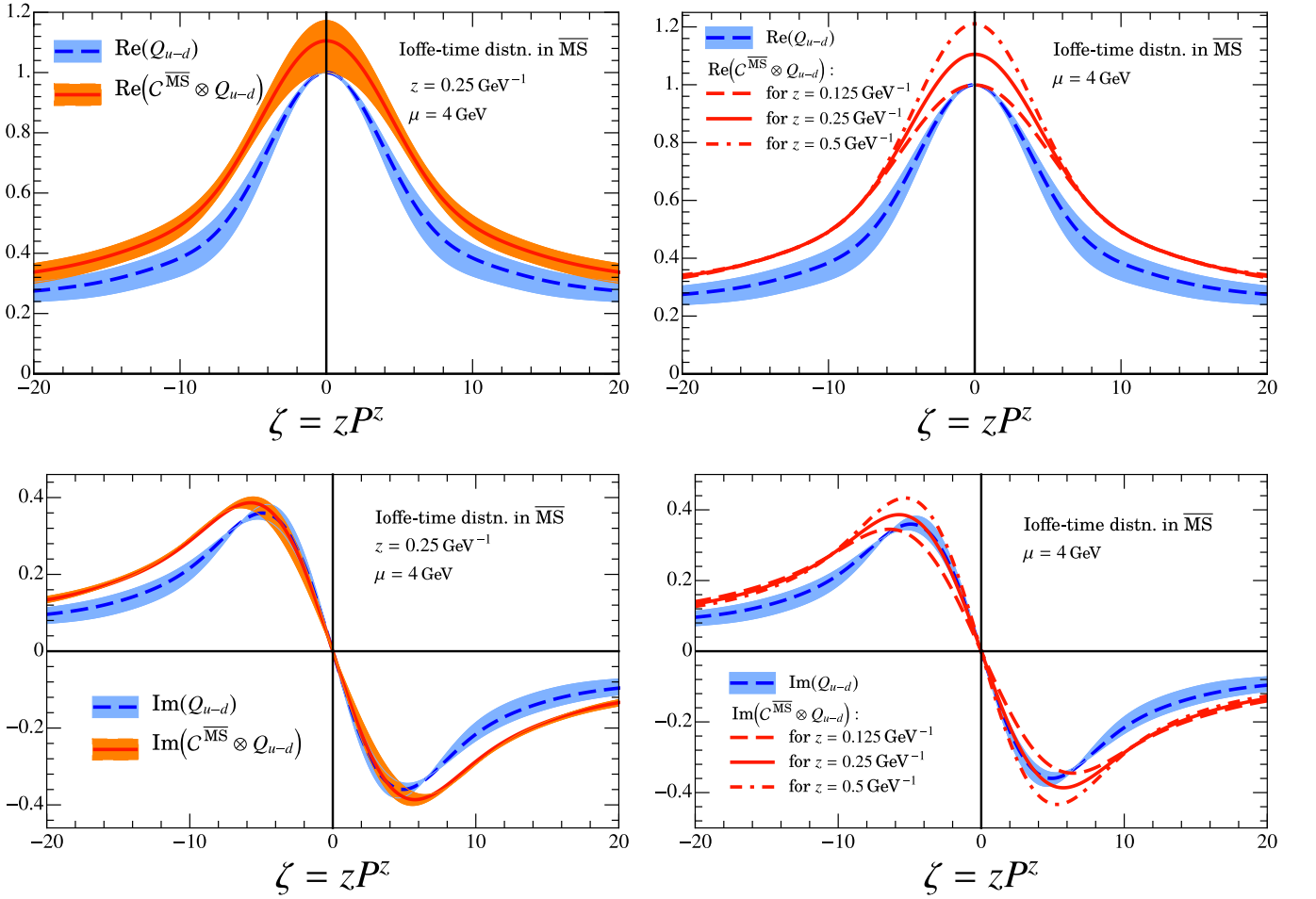


FIG. 4. (left) Comparison between the light-cone time distribution  $Q_{u-d}$  and Ioffe-time distribution from  $(C^{\overline{\text{MS}}} \otimes Q_{u-d})$  in the  $\overline{\text{MS}}$  scheme. The orange and blue bands indicate the results from varying the factorization scale  $\mu = 4 \text{ GeV}$  by a factor of two. (right) Same but now showing only central Ioffe-time curves for different values of  $z$ . The top panels show the real part, while bottom panels show the imaginary part.

to satisfy  $z\Lambda_{\text{QCD}} \ll 1$  and  $P^z \gg \Lambda_{\text{QCD}}$ , we must have

$$m \ll 11, \quad n \gg 1. \quad (83)$$

To control the higher-twist correction at 20%, i.e.  $z^2\Lambda_{\text{QCD}}^2 = 0.2$ ,  $\Lambda_{\text{QCD}}^2/P_z^2 = 0.2$ , we can only choose

$$m = \{0, 1, 2, 3, 4\}, \quad n = \{3, 4, 5, 6, \dots\}, \quad (84)$$

where the largest value for  $n$  is limited by what is practical in current lattice simulations. 6 is the largest number of units attained in Ref. [42]. For quasi-PDF calculations, there are  $4 \times 2 + 1 = 9$  useful data points for each fixed momentum  $|P^z|$ ; for pseudo-PDF calculation, there are only  $4 \times 2 = 8$  useful data points for each fixed  $|z|$ . In either case, it is anticipated that a direct Fourier transform with respect to  $z$  or  $\zeta = zP^z$  will lead to oscillation in  $x$ -space and incorrect prediction for the small- $x$  region due to the truncation in coordinate space. This has been observed in a recent lattice calculation of the quasi-PDF in Ref. [34]. Methods have been developed in recent works to eliminate the oscillation from the truncation effect [35, 61] in the quasi-PDF, but the higher-twist

contributions at large  $z$  still needs to be systematically corrected.

To fully take advantage of all the useful data points, we can evolve them to either the same  $z^2$  or  $P^z$  according to the perturbative analysis, which has been studied in Refs. [42, 43, 53] for the Ioffe-time distribution. However, since the evolution equation of the Ioffe-time distribution in  $\ln z^2$  or  $\ln P_z^2$  follows a nonlocal convolution in  $\zeta = zP^z$  or  $z$ , one has to know the full information in coordinate space to do the evolution. With limited number of data points, either large uncertainties or adopting a model-dependent assumption about the shape is inevitable.

To improve the precision of either approach, the only way forward is to have finer lattice spacing  $a$  so that we could have more data points which satisfy  $z \ll \Lambda_{\text{QCD}}^{-1}$  and larger nucleon momentum  $P^z$ . With increasing  $P^z$ , the valence distribution of the nucleon is contracted in the  $z$  direction, so the spatial correlation of valence quarks is shrunk into smaller distance in  $z$ . If  $P^z$  is large enough, the spatial correlation will fall off quickly within

$z < \Lambda_{\text{QCD}}^{-1}$ , then the truncation error from Fourier transform will be significantly reduced. On the other hand, if we interpret the spatial correlation as the Ioffe-time distribution, its shape will not change under a Lorentz boost because it is a scalar function of  $\zeta = zP^z$  and  $z^2$ . Nevertheless, finer lattice spacing  $a$  allows for calculation with a wider range of  $P^z$ , thus covering larger values of the Ioffe-time  $\zeta = zP^z$  to reduce the truncation error. Since the number of useful data points increases quadratically with  $1/a$ , a more precise lattice calculation with controlled systematic errors will be available in the future.

## VII. CONCLUSIONS

We have proven factorization theorems for the quasi-PDF, Ioffe-time distribution and pseudo PDF using an operator product expansion for the gauge-invariant space-like quark Wilson line operator. The three Euclidean distribution functions are related observables, and all follow from the same fundamental factorization theorem. For the Ioffe-time distribution this proof implies that the ratio in Eq. (34) does scale in  $z^2$ , but needs the small  $z^2$  factorization formula in Eq. (23) to extract the PDF. Our proof for the factorization formula applies when the renormalized Ioffe-time distribution is defined in any scheme. Note that LaMET is not equivalent to the expansion from the OPE, as the former is more general and can be applied to the lattice calculations of other quantities, for example the TMD-PDF where a simple OPE does not exist.

Our derivation of the factorization theorem for the quasi-PDF also verifies that the parton momentum  $p^z$  in the matching coefficient in Eq. (6) has to be  $\underline{p^z} = yP^z$ , which makes a considerable difference for the  $\overline{\text{MS}}$  matching result when compared with  $p^z = P^z$  (see Fig. 2). The proper  $p^z$  should therefore be used in lattice calculations of the PDF in the LaMET approach. In comparing the quasi-PDF and pseudo-PDF it is interesting to note that  $x$  moments of the pseudo-PDF at finite  $z$  exist and factor into short and long-distance pieces (see Eq. (31)), whereas higher  $x$  moments of the quasi-PDF are divergent. This makes it interesting to consider using the pseudo-PDF together with lattice results for the PDF moments.

As a non-trivial test of relations between the various distributions and factorization theorems we considered results at one-loop in the  $\overline{\text{MS}}$  scheme. We derived a corrected results for the coefficient  $C$  for the  $\overline{\text{MS}}$  scheme, given in Eq. (67), which leads to convergent results in the convolution integral. We also computed the one-loop  $\overline{\text{MS}}$  result for the Wilson coefficient  $\mathcal{C}$  appearing in the Ioffe-time and pseudo-PDF factorization theorems. A numerical analysis of these one-loop corrections in  $\overline{\text{MS}}$  was also provided. The one-loop matching coefficient  $\mathcal{C}$  has a smaller effect for the pseudo-PDF than  $C$  does for quasi-PDF, as can be seen by comparing Figs. 2 and 3.

There are several different ways of implementing the factorization theorem to calculate the PDF from lattice data for the Ioffe-time distribution  $\tilde{Q}$ , which we discussed in Sec. VI. One always has to work with short distance correlation and large nucleon momentum to reduce higher-twist corrections. This limits the number of useful data points from lattice calculations as described in Sec. VI. To achieve precision calculations without making model assumptions it will be highly desirable to move to finer lattice spacing to increase the number of effective data points.

## ACKNOWLEDGMENT

The authors are thankful for discussions with J. H. Zhang and Y. B. Yang. This material was partially supported by the U.S. Department of Energy, Office of Science, Office of Nuclear Physics from DE-FG02-93ER-40762, DE-SC0011090 and DE-SC0012704, by the Laboratory Directed Research and Development (LDRD) funding of BNL under contract DE-EC0012704, by a grant from the National Science Foundation of China (No. 11405104), and within the framework of the TMD Topical Collaboration. I.S. was also supported in part by the Simons Foundation through the Investigator grant 327942. T.I. was also supported by JSPS KAKENHI Grant Numbers JP26400261, JP17H02906, and also MEXT as Priority Issue on Post-K computer (Elucidation of the Fundamental Laws and Evolution of the Universe) and JICFuS.

## Appendix A: Fourier Transform

To Fourier transform the bare pseudo-PDF in Eq. (45) into the bare quasi-PDF, we use the identity

$$\begin{aligned}
 & \int \frac{d\zeta}{2\pi} e^{ix\zeta} (z^2 \mu^2)^\epsilon \Gamma(-\epsilon) 4^{-\epsilon} \\
 &= \left(\frac{\mu^2}{p_z^2}\right)^\epsilon \int \frac{d\zeta}{2\pi} e^{ix\zeta} \int_0^\infty d\alpha \alpha^{-1-\epsilon} e^{-\alpha\zeta^2} 4^{-\epsilon} \\
 &= \left(\frac{\mu^2}{p_z^2}\right)^\epsilon \int_0^\infty \frac{d\alpha}{2\sqrt{\pi}} \alpha^{-3/2-\epsilon} e^{-x^2/(4\alpha)} 4^{-\epsilon} \\
 &= \left(\frac{\mu^2}{p_z^2}\right)^\epsilon \frac{\Gamma(\epsilon + 1/2)}{\sqrt{\pi}} \frac{1}{|x|^{1+2\epsilon}}, \tag{A1}
 \end{aligned}$$

which is true for  $\epsilon < 0$ .

Now let us turn to a plus function  $g(y)_{+(1)}^{[0,1]}$ . The double

Fourier transform

$$\begin{aligned}
& \int \frac{d\zeta}{2\pi} e^{ix\zeta} \int_0^1 dy e^{-iy\zeta} g(y)_{+(1)}^{[0,1]} (z^2 \mu^2)^\epsilon \Gamma(-\epsilon) 4^{-\epsilon} \\
&= (i\zeta) \int \frac{d\zeta}{2\pi} e^{i(x-1)\zeta} \int_0^1 dy \int_0^1 dt y g(1-y) \\
&\quad \times e^{ity\zeta} (z^2 \mu^2)^\epsilon \Gamma(-\epsilon) 4^{-\epsilon} \\
&= \left( \frac{\mu^2}{p_z^2} \right)^\epsilon \frac{\Gamma(\epsilon + \frac{1}{2})}{\sqrt{\pi}} \frac{\partial}{\partial x} \int_0^1 dy \int_0^1 dt \frac{y g(1-y)}{|x-y|^{1+2\epsilon}}. \quad (\text{A2})
\end{aligned}$$

Since the integration over  $y$  and  $t$  leads to a piecewise

function of  $x$ , the derivative will end up with a plus function as the discontinuity at  $x = 1$  gives  $\delta(1-x)$ .

## Appendix B: Quasi-PDF Calculation

Here we quote the pure dimensional regularization results obtained when we carry out the quasi-PDF calculation following Refs. [24, 26] by Fourier transforming from  $z$  to  $xp^z$  for the integrand to obtain  $[\delta(p^z - xp^z) - \delta(k^z - xp^z)]$ . For the vertex and wavefunction renormalization graphs we obtain

$$\begin{aligned}
& \tilde{q}_{\text{vertex}}^{(1)}(x, p^z, \epsilon) + \tilde{q}_{\text{w.fn.}}^{(1)}(x, p^z, \epsilon) \\
&= \frac{\alpha_s C_F}{2\pi} \left( \frac{\mu^2}{p_z^2} \right)^\epsilon \left[ (1-\epsilon) \int_0^1 dy (1-y) \frac{1}{|x-y|^{1+2\epsilon}} \frac{\Gamma(\epsilon + \frac{1}{2})}{\sqrt{\pi}} - \delta(1-x) \frac{1}{2} \left( \frac{1}{\epsilon_{\text{UV}}} - \frac{1}{\epsilon_{\text{IR}}} \right) \right], \quad (\text{B1})
\end{aligned}$$

while for the sail diagram

$$\begin{aligned}
& \tilde{q}_{\text{sail}}^{(1)}(x, p^z, \epsilon) \\
&= \frac{\alpha_s C_F}{2\pi} \left( \frac{4\pi\mu^2}{p_z^2} \right)^\epsilon \left[ \int_0^1 dy \frac{x+y}{1-x} \frac{1}{|x-y|^{1+2\epsilon}} \frac{\Gamma(\epsilon + \frac{1}{2})}{\sqrt{\pi}} - \delta(1-x) \int dx' \int_0^1 dy \frac{x'+y}{1-x'} \frac{1}{|x'-y|^{1+2\epsilon}} \frac{\Gamma(\epsilon + \frac{1}{2})}{\sqrt{\pi}} \right] \\
&= \frac{\alpha_s C_F}{2\pi} \left( \frac{\mu^2}{p_z^2} \right)^\epsilon \left[ \int_0^1 dy \frac{x+y}{1-x} \frac{1}{|x-y|^{1+2\epsilon}} \frac{\Gamma(\epsilon + \frac{1}{2})}{\sqrt{\pi}} + \delta(1-x) \left( \frac{1}{\epsilon_{\text{UV}}} - \frac{1}{\epsilon_{\text{IR}}} \right) \right. \\
&\quad \left. - \delta(1-x) \int dx' \int_0^1 dy \frac{1+y}{1-x'} \frac{1}{|x'-y|^{1+2\epsilon}} \frac{\Gamma(\epsilon_{\text{IR}} + \frac{1}{2})}{\sqrt{\pi}} \right], \quad (\text{B2})
\end{aligned}$$

and for the tadpole diagram

$$\begin{aligned}
& \tilde{q}_{\text{tadpole}}^{(1)}(x, p^z, \epsilon) \\
&= \frac{\alpha_s C_F}{2\pi} \left( \frac{4\pi\mu^2}{p_z^2} \right)^\epsilon \left[ -\frac{1}{1-2\epsilon} \frac{1}{|1-x|^{1+2\epsilon}} \frac{\Gamma(\epsilon + \frac{1}{2})}{\sqrt{\pi}} - \delta(1-x) \frac{1}{1-2\epsilon} \frac{1}{|1-x|^{1+2\epsilon}} \int_{-\infty}^{\infty} dx' \frac{1}{|1-x'|^{1+2\epsilon}} \frac{\Gamma(\epsilon + \frac{1}{2})}{\sqrt{\pi}} \right] \\
&= \frac{\alpha_s C_F}{2\pi} \left( \frac{4\pi\mu^2}{p_z^2} \right)^\epsilon \left[ -\frac{1}{1-2\epsilon} \frac{1}{|1-x|^{1+2\epsilon}} \frac{\Gamma(\epsilon + \frac{1}{2})}{\sqrt{\pi}} + \delta(1-x) \left( \frac{1}{\epsilon_{\text{UV}}} - \frac{1}{\epsilon_{\text{IR}}} \right) \right]. \quad (\text{B3})
\end{aligned}$$

After adding these expressions and carrying out the remaining integrations over  $y$ , we obtain the same result as in Eq. (47).

## Appendix C: $\epsilon$ Expansion and Plus Functions

Since the support of the quasi-PDF ranges from  $-\infty$  to  $\infty$ , its asymptotic behavior as  $\sim 1/|x|$  at  $|x| \rightarrow \infty$  implies a UV divergence which can be regularized by dimensional regularization. Therefore, the  $\epsilon$  expansion of the quasi-PDF should account for this feature.

In general, we need to expand

$$\frac{\theta(x)}{x^{1+\epsilon}} = \frac{\theta(x)\theta(1-x)}{x^{1+\epsilon}} + \frac{\theta(x-1)}{x^{1+\epsilon}}, \quad (\text{C1})$$

and it is well known that

$$\frac{\theta(x)\theta(1-x)}{x^{1+\epsilon}} = -\frac{1}{\epsilon} \delta(x) + \tilde{\mathcal{L}}_0(x) - \epsilon \tilde{\mathcal{L}}_1(x) + O(\epsilon^2), \quad (\text{C2})$$

where  $\epsilon < 0$ . Here we follow [62] and the plus functions  $\mathcal{L}_n(x)$  are defined as

$$\begin{aligned}
\mathcal{L}_n(x) &\equiv \left[ \frac{\theta(x) \ln^n x}{x} \right]_+ \\
&= \lim_{\beta \rightarrow 0} \left[ \frac{\theta(x-\beta) \ln^n x}{x} + \delta(x-\beta) \frac{\ln^{n+1} \beta}{n+1} \right], \quad (\text{C3})
\end{aligned}$$

and we let

$$\tilde{\mathcal{L}}_n(x) = \theta(1-x) \mathcal{L}_n(x). \quad (\text{C4})$$

Note that  $\int_0^1 dx \mathcal{L}_n(x) = 0$ .

To define the expansion in the range  $x \in [1, \infty]$  we simply map this interval to  $[0, 1]$  via  $t = 1/x$ . Taking an arbitrary smooth test function  $g(x)$  we have

$$\begin{aligned} & \int_1^\infty dx \frac{1}{x^{1+\epsilon}} g(x) \\ &= \int_0^1 dt \frac{1}{t^{1-\epsilon}} g(1/t) \\ &= \int_0^1 dt \left[ \frac{1}{\epsilon} \delta(t) + \mathcal{L}_0(t) + \epsilon \mathcal{L}_1(t) + O(\epsilon^2) \right] g(1/t) \\ &= \int_1^\infty \frac{dx}{x^2} \left[ \frac{1}{\epsilon} \delta^+ \left( \frac{1}{x} \right) + \mathcal{L}_0 \left( \frac{1}{x} \right) + \epsilon \mathcal{L}_1 \left( \frac{1}{x} \right) + O(\epsilon^2) \right] g(x). \end{aligned} \quad (\text{C5})$$

Here  $\epsilon > 0$  and the superscript  $+$  on the  $\delta^+$  function indicates that its argument should be positive. Therefore  $\delta^+(1/x)$  has its support at  $x = +\infty$ , not  $x = -\infty$ . Since  $g$  is arbitrary we can identify

$$\begin{aligned} \frac{\theta(x-1)}{x^{1+\epsilon}} &= \frac{1}{\epsilon} \frac{1}{x^2} \delta^+ \left( \frac{1}{x} \right) + \frac{1}{x^2} \tilde{\mathcal{L}}_0 \left( \frac{1}{x} \right) + \epsilon \frac{1}{x^2} \tilde{\mathcal{L}}_1 \left( \frac{1}{x} \right) \\ &\quad + O(\epsilon^2). \end{aligned} \quad (\text{C6})$$

Combining the above results and denoting which  $1/\epsilon$  poles are UV or IR divergences we have

$$\begin{aligned} \frac{\theta(x)}{x^{1+\epsilon}} &= \left[ -\frac{1}{\epsilon_{\text{IR}}} \delta(x) + \frac{1}{\epsilon_{\text{UV}}} \frac{1}{x^2} \delta^+ \left( \frac{1}{x} \right) \right] \\ &\quad + \left( \frac{1}{x} \right)_{+(0)}^{[0,1]} + \left( \frac{1}{x} \right)_{+(\infty)}^{[1,\infty]} \\ &\quad - \epsilon \left[ \left( \frac{\ln x}{x} \right)_{+(0)}^{[0,1]} + \left( \frac{\ln x}{x} \right)_{+(\infty)}^{[1,\infty]} \right] + O(\epsilon^2), \end{aligned} \quad (\text{C7})$$

where we have defined the distributions

$$(1/x)_{+(0)}^{[0,1]} \equiv \tilde{\mathcal{L}}_0(x), \quad (\ln x/x)_{+(0)}^{[0,1]} \equiv \tilde{\mathcal{L}}_1(x), \quad (\text{C8})$$

and

$$\begin{aligned} (1/x)_{+(\infty)}^{[1,\infty]} &\equiv (1/x^2) \tilde{\mathcal{L}}_0(1/x), \\ (\ln x/x)_{+(\infty)}^{[1,\infty]} &\equiv -(1/x^2) \tilde{\mathcal{L}}_1(1/x). \end{aligned} \quad (\text{C9})$$

Note that Eq. (C7) is consistent with the expected result that

$$\int_0^\infty \frac{dx}{x^{1+\epsilon}} = \frac{1}{\epsilon_{\text{UV}}} - \frac{1}{\epsilon_{\text{IR}}}. \quad (\text{C10})$$

- 
- [1] J. C. Collins, D. E. Soper, and G. F. Sterman, *Adv. Ser. Direct. High Energy Phys.* **5**, 1 (1989), arXiv:hep-ph/0409313 [hep-ph].
- [2] R. D. Ball *et al.* (NNPDF), *JHEP* **04**, 040 (2015), arXiv:1410.8849 [hep-ph].
- [3] S. Dulat, T.-J. Hou, J. Gao, M. Guzzi, J. Huston, P. Nadolsky, J. Pumplin, C. Schmidt, D. Stump, and C. P. Yuan, *Phys. Rev.* **D93**, 033006 (2016), arXiv:1506.07443 [hep-ph].
- [4] A. D. Martin, W. J. Stirling, R. S. Thorne, and G. Watt, *Eur. Phys. J.* **C63**, 189 (2009), arXiv:0901.0002 [hep-ph].
- [5] S. Alekhin, J. Blümlein, S. Moch, and R. Placakyte, (2017), arXiv:1701.05838 [hep-ph].
- [6] A. Buckley, J. Ferrando, S. Lloyd, K. Nordström, B. Page, M. Rüfenacht, M. Schönherr, and G. Watt, *Eur. Phys. J.* **C75**, 132 (2015), arXiv:1412.7420 [hep-ph].
- [7] G. Martinelli and C. T. Sachrajda, *Phys. Lett.* **B196**, 184 (1987).
- [8] G. Martinelli and C. T. Sachrajda, *Phys. Lett.* **B217**, 319 (1989).
- [9] W. Detmold, W. Melnitchouk, and A. W. Thomas, *Eur. Phys. J.direct* **3**, 13 (2001), arXiv:hep-lat/0108002 [hep-lat].
- [10] W. Detmold, W. Melnitchouk, and A. W. Thomas, *Phys. Rev.* **D66**, 054501 (2002), arXiv:hep-lat/0206001 [hep-lat].
- [11] D. Dolgov *et al.* (LHPC, TXL), *Phys. Rev.* **D66**, 034506 (2002), arXiv:hep-lat/0201021 [hep-lat].
- [12] Z. Davoudi and M. J. Savage, *Phys. Rev.* **D86**, 054505 (2012), arXiv:1204.4146 [hep-lat].
- [13] K.-F. Liu and S.-J. Dong, *Phys. Rev. Lett.* **72**, 1790 (1994), arXiv:hep-ph/9306299 [hep-ph].
- [14] K. F. Liu, S. J. Dong, T. Draper, D. Leinweber, J. H. Sloan, W. Wilcox, and R. M. Woloshyn, *Phys. Rev.* **D59**, 112001 (1999), arXiv:hep-ph/9806491 [hep-ph].
- [15] K.-F. Liu, *Phys. Rev.* **D62**, 074501 (2000), arXiv:hep-ph/9910306 [hep-ph].
- [16] K.-F. Liu, *Proceedings, 33rd International Symposium on Lattice Field Theory (Lattice 2015): Kobe, Japan, July 14-18, 2015*, PoS **LATTICE2015**, 115 (2016), arXiv:1603.07352 [hep-ph].
- [17] A. J. Chambers, R. Horsley, Y. Nakamura, H. Perlt, P. E. L. Rakow, G. Schierholz, A. Schiller, K. Somfleth, R. D. Young, and J. M. Zanotti, *Phys. Rev. Lett.* **118**,

- 242001 (2017), arXiv:1703.01153 [hep-lat].
- [18] W. Detmold and C. J. D. Lin, Phys. Rev. **D73**, 014501 (2006), arXiv:hep-lat/0507007 [hep-lat].
- [19] Y.-Q. Ma and J.-W. Qiu, (2014), arXiv:1404.6860 [hep-ph].
- [20] Y.-Q. Ma and J.-W. Qiu, (2017), arXiv:1709.03018 [hep-ph].
- [21] X. Ji, Phys. Rev. Lett. **110**, 262002 (2013), arXiv:1305.1539 [hep-ph].
- [22] X. Ji, Sci. China Phys. Mech. Astron. **57**, 1407 (2014), arXiv:1404.6680 [hep-ph].
- [23] Y. Hatta, X. Ji, and Y. Zhao, Phys. Rev. **D89**, 085030 (2014), arXiv:1310.4263 [hep-ph].
- [24] X. Xiong, X. Ji, J.-H. Zhang, and Y. Zhao, Phys. Rev. **D90**, 014051 (2014), arXiv:1310.7471 [hep-ph].
- [25] C. Alexandrou, K. Cichy, V. Drach, E. Garcia-Ramos, K. Hadjiyiannakou, K. Jansen, F. Steffens, and C. Wiese, Phys. Rev. **D92**, 014502 (2015), arXiv:1504.07455 [hep-lat].
- [26] I. W. Stewart and Y. Zhao, (2017), arXiv:1709.04933 [hep-ph].
- [27] W. Wang, S. Zhao, and R. Zhu, (2017), arXiv:1708.02458 [hep-ph].
- [28] W. Wang and S. Zhao, (2017), arXiv:1712.09247 [hep-ph].
- [29] H.-W. Lin, J.-W. Chen, S. D. Cohen, and X. Ji, Phys. Rev. **D91**, 054510 (2015), arXiv:1402.1462 [hep-ph].
- [30] J.-W. Chen, S. D. Cohen, X. Ji, H.-W. Lin, and J.-H. Zhang, Nucl. Phys. **B911**, 246 (2016), arXiv:1603.06664 [hep-ph].
- [31] C. Alexandrou, K. Cichy, M. Constantinou, K. Hadjiyiannakou, K. Jansen, F. Steffens, and C. Wiese, Phys. Rev. **D96**, 014513 (2017), arXiv:1610.03689 [hep-lat].
- [32] J.-H. Zhang, J.-W. Chen, X. Ji, L. Jin, and H.-W. Lin, Phys. Rev. **D95**, 094514 (2017), arXiv:1702.00008 [hep-lat].
- [33] C. Alexandrou, K. Cichy, M. Constantinou, K. Hadjiyiannakou, K. Jansen, H. Panagopoulos, and F. Steffens, Nucl. Phys. **B923**, 394 (2017), arXiv:1706.00265 [hep-lat].
- [34] J.-W. Chen, T. Ishikawa, L. Jin, H.-W. Lin, Y.-B. Yang, J.-H. Zhang, and Y. Zhao, (2017), arXiv:1706.01295 [hep-lat].
- [35] H.-W. Lin, J.-W. Chen, T. Ishikawa, and J.-H. Zhang, (2017), arXiv:1708.05301 [hep-lat].
- [36] J.-W. Chen, L. Jin, H.-W. Lin, A. Schfer, P. Sun, Y.-B. Yang, J.-H. Zhang, R. Zhang, and Y. Zhao, (2017), arXiv:1712.10025 [hep-ph].
- [37] H.-W. Lin *et al.*, (2017), arXiv:1711.07916 [hep-ph].
- [38] X. Ji, A. Schäfer, X. Xiong, and J.-H. Zhang, Phys. Rev. **D92**, 014039 (2015), arXiv:1506.00248 [hep-ph].
- [39] A. V. Radyushkin, Phys. Rev. **D96**, 034025 (2017), arXiv:1705.01488 [hep-ph].
- [40] A. V. Radyushkin, Phys. Lett. **131B**, 179 (1983).
- [41] A. Radyushkin, Phys. Lett. **B767**, 314 (2017), arXiv:1612.05170 [hep-ph].
- [42] K. Orginos, A. Radyushkin, J. Karpie, and S. Zafeiropoulos, (2017), arXiv:1706.05373 [hep-ph].
- [43] J. Karpie, K. Orginos, A. Radyushkin, and S. Zafeiropoulos, (2017), arXiv:1710.08288 [hep-lat].
- [44] X. Ji, J.-H. Zhang, and Y. Zhao, (2017), arXiv:1706.07416 [hep-ph].
- [45] Y. Zhao, *Factorization Theorem Relating Euclidean and Light-Cone Parton Distributions* (Talk given at INT Workshop 17-68W, “Flavor Structure of the Nucleon Sea”, Seattle, US, 2017).
- [46] X. Ji, J.-H. Zhang, and Y. Zhao, (2017), arXiv:1706.08962 [hep-ph].
- [47] T. Ishikawa, Y.-Q. Ma, J.-W. Qiu, and S. Yoshida, (2017), arXiv:1707.03107 [hep-ph].
- [48] O. Nachtmann, Nucl. Phys. **B63**, 237 (1973).
- [49] V. Braun and D. Mueller, Eur. Phys. J. **C55**, 349 (2008), arXiv:0709.1348 [hep-ph].
- [50] G. S. Bali, V. M. Braun, M. Gckeler, M. Gruber, F. Hutzler, P. Korcyl, B. Lang, A. Schfer, P. Wein, and J.-H. Zhang, in *35th International Symposium on Lattice Field Theory (Lattice 2017) Granada, Spain, June 18-24, 2017* (2017) arXiv:1709.04325 [hep-lat].
- [51] M. Constantinou and H. Panagopoulos, (2017), arXiv:1705.11193 [hep-lat].
- [52] J.-H. Zhang, J.-W. Chen, and C. Monahan, (2018), arXiv:1801.03023 [hep-ph].
- [53] A. V. Radyushkin, (2017), arXiv:1710.08813 [hep-ph].
- [54] A. Radyushkin, (2018), arXiv:1801.02427 [hep-ph].
- [55] X. Ji and J.-H. Zhang, Phys. Rev. **D92**, 034006 (2015), arXiv:1505.07699 [hep-ph].
- [56] T. Ishikawa, Y.-Q. Ma, J.-W. Qiu, and S. Yoshida, (2016), arXiv:1609.02018 [hep-lat].
- [57] J.-W. Chen, X. Ji, and J.-H. Zhang, Nucl. Phys. **B915**, 1 (2017), arXiv:1609.08102 [hep-ph].
- [58] X. Xiong, T. Luu, and U.-G. Meißner, (2017), arXiv:1705.00246 [hep-ph].
- [59] J. Green, K. Jansen, and F. Steffens, (2017), arXiv:1707.07152 [hep-lat].
- [60] J.-W. Chen, T. Ishikawa, L. Jin, H.-W. Lin, Y.-B. Yang, J.-H. Zhang, and Y. Zhao, (2017), arXiv:1710.01089 [hep-lat].
- [61] J.-H. Zhang and et al., (2017), in preparation.
- [62] Z. Ligeti, I. W. Stewart, and F. J. Tackmann, Phys. Rev. **D78**, 114014 (2008), arXiv:0807.1926 [hep-ph].